NASA CONTRACTOR REPORT

NASA CR-481

NASA CR-481

NUMERICAL CALCULATIONS OF GAS-SURFACE INTERACTIONS

by Richard A. Oman

Prepared by
GRUMMAN AIRCRAFT ENGINEERING CORPORATION
Bethpage, N. Y.
for

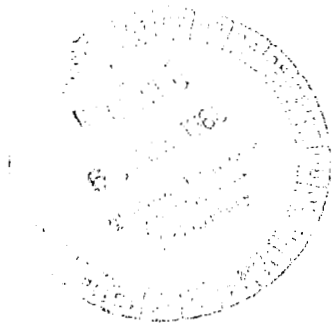

NATIONAL AERONAUTICS AND SPACE ADMINISTRATION • WASHINGTON, D. C. • MAY 1966

NASA CR-481

NUMERICAL CALCULATIONS OF GAS-SURFACE INTERACTIONS

By Richard A. Oman

Prepared under Contract No. NASw-1027 by
GRUMMAN AIRCRAFT ENGINEERING CORPORATION
Bethpage, N.Y.

for

NATIONAL AERONAUTICS AND SPACE ADMINISTRATION

For sale by the Clearinghouse for Federal Scientific and Technical Information
Springfield, Virginia 22151 – Price $3.00

ACKNOWLEDGMENTS

Many people assisted in carrying out this work. I would like to thank particularly Messrs. Alexander Bogan, Jr., Calvin Weiser, and Dr. Chou H. Li, who have participated in many useful discussions, and helped in many ways on this and earlier efforts. I am also grateful for the support and encouragement of many other colleagues in the Grumman Research Department.

ABSTRACT

Numerical calculations of gas-surface interactions at epithermal energies are reported and correlated. These interactions, which involve: the effects of different lattice structures and orientations, adsorbed contaminants, and lattice thermal motion, are compared against those of ideal FCC (100) surfaces at 0°K. An analysis of energy exchange in 153 different situations (including some previously reported) is developed by considering a highly idealized model of the interaction and determining parameters in the model from the complete set of numerical results. The resulting simple equation correlates theoretical energy exchange values with a standard deviation of about 10 per cent of the incident energy for cold ideal surfaces, and about 20 per cent for hot, contaminated surfaces and different structures.

A previous report (Ref. 2) presents evidence for neglecting coupling between lattice oscillators in calculations involving high gas particle energy. The present results lend further support to this approximation. A single monolayer of adsorbed material was found in effect to dominate the interaction in most cases, isolating the gas particle from all but a small, long-range influence of the bulk. Calculations of lattice thermal effects on the interactions, although subject to errors due to small sample size, indicate that this effect can safely be ignored at high incident energy. Lattice surface structure and azimuth angle of incidence were found to be important only in the FCC (110) case, where the surface is quite rough and highly directional.

TABLE OF CONTENTS

LIST OF ILLUSTRATIONS

LIST OF TABLES

LIST OF SYMBOLS

A	correction for attractive potential
a,a', b,c	parameters of interaction
COL	coupled oscillator lattice
d	unit of length (= $\frac{1}{2}$ lattice spacing)
E	energy
F	force
IOL	independent oscillator lattice
k	Boltzmann's constant
m	mass
n	number of lattice atoms/d^3; also number of degrees of freedom of gas particle
p	momentum
T	temperature
x_j	independent variable
α	accommodation coefficient
δ	error measure for optimization
ϵ	depth of Lennard-Jones 6-12 potential
η	fraction of incident flow that is trapped
θ	angle between velocity vector and normal to surface
μ	mass ratio (lattice/gas)
σ	range parameter of Lennard-Jones 6-12 potential
σ_t	tangential momentum accommodation coefficient
σ_z	normal momentum accommodation coefficient (the normalized vectorial normal momentum difference between incident and reflected molecule)
τ	time interval
ϕ	azimuthal angle of velocity
ω	frequency
Ω	dimensionless frequency parameter ($=\omega_n d/V_i$)

Subscripts

b	bulk property
c	collision
f	final state after interaction
g	gas
i	initial state
ℓ	lattice (or solid)
L	lateral ($\parallel$ to surface, but $\perp$ to incident ray)
n	natural frequency of lattice
s	surface property
v	vibration of diatomic molecule
w	wall (temperature)
z_o	reference altitude above surface

Special Notation

$s(y_i)$	standard deviation of y_i
$\bar{F}$	mean of F

INTRODUCTION

References 1 and 2 provide a description of the basic numerical method for calculating molecular trajectories in the vicinity of solid surfaces. Very briefly, we calculate the three dimensional, classical trajectories of gas molecules directed at a crystal lattice that is represented by a set of harmonic oscillators which are point centers of potential (a Lennard-Jones 6-12). The recoil of the oscillators is the mechanism by which energy is transferred to the lattice. Most of the calculations assume that the lattice oscillators are mutually independent. Several other cases, computed for a model in which the lattice atoms are coupled, indicate that the range of reasonable validity for the independent-oscillator lattice (IOL) model is surprisingly large. Momentum and energy exchanges as well as exiting velocity vectors are computed and averaged over many parallel incident trajectories, each having a slightly different aiming point on the lattice surface. A set of exiting molecules is thereby generated to represent the distributions that would result from a perfectly collimated molecular ray of perfectly homogeneous physical properties impinging on the surface.

Reference 1 presents a few typical results obtained from the above method, and describes qualitatively some of the general characteristics of observed behavior. It also describes the first attempt to combine the independent variables of the problem in parametric form, in order to provide a framework for correlating the results. Reference 2 presents the comparison between coupled-and-independent-oscillator models described above, gives the results of statistical correlations of momentum energy and angular spreads from a planned design of 64 cases designed to cover the range of interest, and indicates the energy and angle-of incidence dependence to be expected for He, Ne, and Ar on a (100) face of a Ni lattice.

All of the work described in Refs. 1 and 2 treats a very elementary case, namely, the lattice is initially at rest; the gas molecule is a point mass; the lattice is clean and ideal; its force laws are isotropic (although the atoms are located in a

realistic structure); the intermolecular potential curve is assumed always to have the same shape, and quantum-mechanical effects are ignored. There are some other limitations, but these are probably the most important ones aside from the IOL assumption previously mentioned. Because the primary motivation for this work has been the understanding and characterization of the aerodynamic effects of molecule-surface interactions, the primary concern is with very high thermal energies (0.1-15 ev) and moderately heavy gas particles (10-40 amu), and fairly convincing arguments can be made to justify the above assumptions. A few of the effects could be quite important however, and are also of considerable fundamental interest in their own right. This report and future work will be primarily addressed toward improved characterization of the effects of these complicating factors.

Since the description recorded in Ref. 2, four major capabilities have been added to the family of computer programs: treating crystal planes different from the (100); modeling the effects of adsorbed species by giving the surface layer of atoms physical properties different from those of the lower layers; and portraying the effects of thermal motion in the lattice by a simplified distribution of initial lattice motions. These capabilities open up a truly enormous number of possible cases, and the cases to be computed must be planned carefully so that the results will have over-all meaning. Each of the above modifications will be described, along with the results generated thus far.

There is an additional feature of the theoretical program which is designed to increase the value of the numerical computations. By the analysis of very simple models of interaction processes, a semiempirical correlation equation that predicts quite well the energy exchange given by results of the computer calculations has been derived. This phenomenological approach has the great advantage of giving physical insight into the details of various types of interactions. The approach was first tried in a rough way in Ref. 1, but has since been improved. The latest version is described in this report. It represents an important part of future work because it gives a convenient reference level against which to evaluate the importance of complicating effects, such as internal degrees of freedom.

Correlation with experimental data is vital to the completeness of any theoretical investigation, and this element is thus

far missing in the present study. There are at this time only two sources of data available, although many investigators are actively striving to improve the situation (cf. Refs. 3 and 4). These sources are the thermal cell experiments, best represented by the work of Thomas and his students (cf. Wachman, Ref. 5), and the scattering distributions that have been and are being measured by many investigators in low energy molecular beams (cf. Hurlbut, Ref. 6; Smith and Saltsburg, Ref. 7; and Hinchen and Foley, Ref. 8). Recent reviews by French (Ref. 9), Knuth (Ref. 10), and Anderson, Fenn, and Andres (Ref. 11) describe the many current efforts to make measurements at epithermal energies using arc or shock tube sources, neutralized ion beams, and seeding techniques. There are many problems associated with comparison between the existing data and the theoretical results, but the most important ones are the high wall temperatures (greater than those of the gas) in the thermal cells, and the difficulty in relating measured spatial distributions of flux with a limited sample of exiting molecular trajectories produced by theory. Some attempts being made to bridge these gaps are discussed in the Parametric Analysis Section of this report.

Recent literature on the theory of vibrational energy exchange in gases (Refs. 12 and 13) indicates an increasing confidence in the use of classical mechanics to describe such processes. This fact relates to the present work in two important ways. First, the use of a classical oscillator to portray a diatomic gas molecule seems more reasonable. Second, the mathematical similarities between gas-gas and gas-surface interactions encourage the extension of the same type of arguments to justify definitely the use of classical mechanics in the gas-surface problem. It is clear at this stage that at least two criteria must be fulfilled for classical methods to be valid: 1) the de Broglie wavelength of the incident gas particle must be very much less than the lattice spacing, and 2) the energy exchanged with the lattice in the classical approximation must be large compared to the minimum phonon energy allowed within the real lattice. Both of these criteria are fulfilled above ~ 0.1 ev for atmospheric species and common materials. Quantum mechanics will also be required when electronic excitation in either the lattice or gas particles begins to occur in an appreciable fraction of the molecular impacts. The lower energy boundary for this type of problem is very much dependent on the species involved, but it should be above 10 ev for most cases of interest. It appears that encounters between gas particles and free electrons in the lattice will be unimportant, because the momentum and energy that can be transferred in such a collision is indeed minute.

LATTICE STRUCTURE EFFECTS

One of the most striking results to come out of the 83 cases described in Ref. 2 was the fact that the azimuth angle of incidence, ϕ_i, had only a very small effect on any of the results of physical importance. This was encouraging in two respects: first, it greatly simplifies further studies (both theoretical and experimental) if one of the primary geometric variables is of only minor importance; and second, it leads one to expect that differences in surface structure would similarly prove of little importance to mean values and standard deviations of output quantities, such as energy exchange and momentum accommodation coefficients.

An investigation was conducted to determine if the above preliminary conclusions were correct. The lattice generation logic in the main program was generalized to produce the following crystal configurations:

Body centered cubic (100) and (110)

Simple cubic (100)

Face centered cubic (100), (111), and (110)

Diamond cubic (100)

Hexagonal close-packed (100).

The resulting arrays were plotted and viewed stereoptically as well as checked geometrically. Several runs were made on the principal planes of the FCC structures using different azimuth angles, while all other independent variables were held constant at values expected to maximize the sensitivity of the interactions to ϕ_i. The results of these runs are shown in Figs. 1, 2, and 3. A limited number of runs were also made with each of the other available structures. Table I shows the results of these calculations.

Although the effects of structure and incident azimuth angle do not appear to be of first order importance, there are some definite trends which should be pointed out and explained. First,

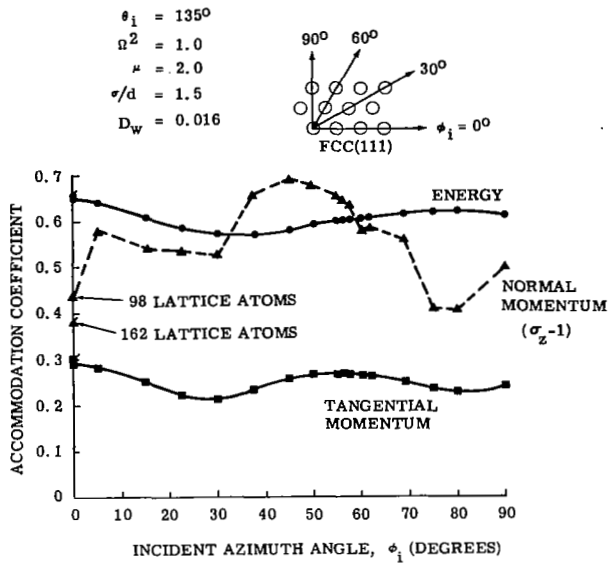

Fig. 1 Effect of Azimuth Angle on FCC (111) Surface

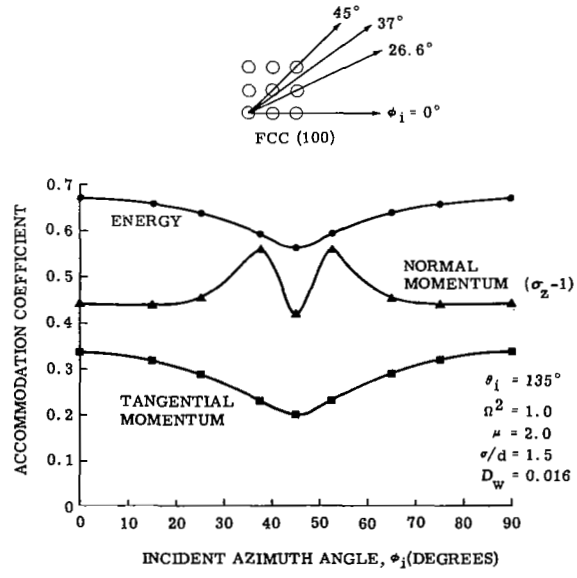

Fig. 2 Effect of Azimuth Angle on FCC (100) Surface

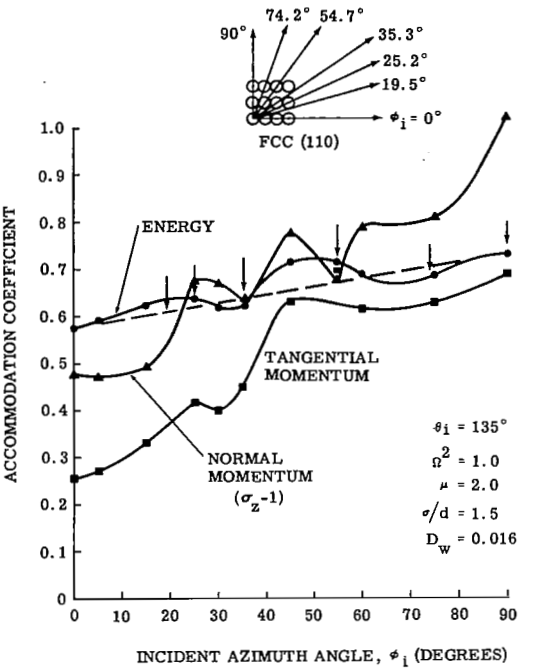

Fig. 3 Effect of Azimuth Angle on FCC (110) Surface

the changes in structure have a much larger effect on momentum than they do on energy exchange. This is to be expected, because momentum exchanges reflect the roughness of the equipotential surfaces felt by the incident particles, whereas energy exchange appears to be controlled mostly by interaction of the incident particle with individual lattice atoms. More will be said on the last point in later sections.

The second major feature in the results is that the closer packed (smoother) surface planes generally showed lower accommodation of energy and tangential momentum. The reverse was true for the normal momentum,* with the exception of the (111) case.

When the azimuth angle changes from a direction of close packing toward one of greater distances between surface atoms, we would expect to see increases in all coefficients of accommodation. This trend is observed quite clearly in the FCC (110) case, but not in the (100) or (111) cases where changes are much less

*Note that in this work the normal momentum coefficient σ_z is somewhat different from Schaaf's σ' in Ref. 14 and is directly proportional to the surface pressure resulting from a prescribed incident momentum flux. The indicated fluctuations in σ_z are probably the result of an insufficient number of trajectories in the samples.

TABLE I

COMPARISON OF RESULTS FOR DIFFERENT LATTICE CONFIGURATIONS

(8 Trajectories Per Case)

	Mean Interaction Parameters						Standard Deviations					
Surface Plane	E_ℓ/E_i	σ_z	σ_L	σ_t	$\cos\theta_f$	$\lvert\Phi_f\rvert$	$s(E_\ell/E_i)$	$s(\sigma_z)$	$s(\sigma_L)$	$s(\sigma_t)$	$s(\cos\theta_f)$	$s(\Phi_f)$
FCC (111)												
Φ_i = 67.5°	0.4826	1.7757	-0.0687	0.1960	0.6154	77.0301	0.0910	0.1838	0.2243	0.2488	0.1458	28.5094
FCC (100)												
Φ_i = 67.5°	0.5242	1.9516	-0.0213	0.6206	0.7549	88.0035	0.1174	0.2746	0.2453	0.4991	0.2178	71.627899
FCC (110)												
Φ_i = 67.5°	0.6121	1.9252	0.0114	0.9273	0.7340	44.3370	0.1446	0.2063	0.2684	0.5452	0.1636	102.463699
BCC (100)												
Φ_i = 67.5°	0.6146	1.8073	0.0030	0.9111	0.6405	16.7120	0.1730	0.2920	0.2621	0.6647	0.2317	102.5463
15°	0.5869	1.8203	-0.0098	0.9557	0.6508	67.2176	0.1820	0.2900	0.2459	0.7113	0.2301	104.2821
BCC (110)												
Φ_i = 67.5°	0.6204	1.8839	-0.1337	0.8581	0.7012	113.3883	0.1490	0.2835	0.1854	0.6136	0.2249	102.3984
15°	0.5529	1.7415	-0.0019	0.5963	0.5883	10.3820	0.1752	0.3412	0.2608	0.6603	0.2707	92.9806
SC (100)												
Φ_i = 67.5°	0.4505	1.8530	-0.0078	0.1619	0.6767	69.2130	0.0941	0.1668	0.1345	0.1951	0.1323	15.48541
15°	0.4482	1.8498	0.0073	0.1568	0.6742	13.4201	0.09148	0.1567	0.1395	0.1856	0.1243	16.0373
DC (100)												
Φ_i = 67.5°	0.6357	1.9014	-0.2098	0.9516	0.7151	178.7142	0.2021	0.1095	0.1550	0.5927	0.0869	59.2478
15°	0.5999	1.6523	0.2225	0.8043	0.5175	-86.0119	0.2154	0.2800	0.1702	0.7730	0.2221	66.1951
HCP (100												
Φ_i = 67.5°	0.4825	1.7756	-0.0687	0.1959	0.6153	77.0311	0.0910	0.1838	0.2243	0.2488	0.1458	28.5033
15°	0.4576	1.7477	0.0121	0.1334	0.5932	13.965	0.0842	0.1637	0.2327	0.1669	0.1299	24.2309

Notes: 1. Azimuth angle (Φ_i) is measured from direction of closest packing except BCC (100), SC (100), and DC (100) where $\Phi_i = 0$ is edge of unit cell.

2. Independent variables are:

$$\Omega^2 = \frac{\omega_n d^2}{V_i} = 3.162 \quad \sigma/d = 1.375 \quad \theta_i = 135°$$

$$\epsilon/E_i = 0.008 \quad m_\ell/m_g = 2.818$$

3. Momentum Parameters:

σ_z = Total Normal Momentum Exchanged/Incident Normal Momentum

σ_L = Net Lateral Momentum/Incident Momentum

σ_t = Tangential Momentum Exchanged/Incident Tangential Momentum

noticeable. The lower energy and tangential momentum exchanges shown for the SC (100) case can be explained in the same way, because the number of lattice atoms per volume d^3 is highest for that structure ($n_{sc} = 1$, $n_{fcc} = \frac{1}{2}$, $n_{bcc} = \frac{1}{4}$, $n_{dc} = \frac{1}{8}$) and all cases in Table I were computed with $\sigma/d = 1.375$.

ADSORBED SURFACE LAYERS

It has been known for some time that the presence of surface contaminants has had an overriding effect on the validity of most of the existing data taken in gas surface interactions (cf. Wachman, Ref. 5). Recent experience with molecular trajectories has reaffirmed these facts and helped to clarify the mechanisms by which the adsorbed species can produce these large effects.

A model was devised to portray adsorbed species on an ideal substrate surface. It has thus far been restricted to complete monolayers, although it is hoped in later work to treat a few types of partial coverage geometries. Physical properties were introduced for the top layer of atoms, which were independent of those of the bulk atoms. The binding energy between bulk and substrate is therefore reflected in the spring constant (Einstein frequency) of the top layer of atoms, while surface and bulk atoms each interact with the gas particle by independent Lennard-Jones 6-12 potentials.

The adsorbed contaminant model has been used in a few screening runs and in a balanced design of 16 cases. The design has the same surface property pattern as used in Ref. 2 for uniform crystals, while bulk properties were quite different. (Initial lattice thermal motion was also included in this plan, as described in the following section.) The differences in results between corresponding cases were then analyzed. A correlation of the differences is shown in Table II and the data are given in the Appendix as runs 84 through 99.

With the exception of a few special situations, the results indicate that the uppermost layer dominates the energy exchange, and plays a very large part in momentum exchanges. This over-all conclusion indicates that the properties of the adsorbate and its bond to the bulk should prove much more important to the interaction than the properties of the bulk. This is true even for

TABLE II

CORRELATION COEFFICIENTS FOR DIFFERENCES BETWEEN MATCHED CASES

SHOWING EFFECTS OF ADSORBED CONTAMINANTS AND LATTICE MOTION

(16 Pairs in Which Surface Properties and Incident Geometries Coincide, But Bulk Properties are Different and Lattice Temperature is Introduced)

		BULK PROPERTIES				INCIDENT GEOMETRY			SURFACE PROPERTIES						LATTICE TEMPERATURE	
Diff. in Output Level (ΔY_i)	Mean Diff. in Output Level $(\bar{Y}_i)$	$\ell n(\Omega_b^2)$	$(\sigma/d)_b$	$\ell n(\epsilon/E_i)_b$	$\ell n(m_b/m_g)$	θ_i Lin.	θ_i Quad.	ϕ_i	$\ell n(\Omega_s^2)$ Lin.	$\ell n(\Omega_s^2)$ Quad.	$(\sigma/d)_s$	$\ell n(\epsilon/E_i)_s$ Lin.	$\ell n(\epsilon/E_i)_s$ Quad.	$\ell n(m_s/m_g)$	$\ell n \frac{3kT_w}{E_i}$ Lin.	$\ell n \frac{3kT_w}{E_i}$ Quad.
$\Delta(\bar{E}_g/E_i)$	-0.292	-0.005	0.103	-0.068	0.041	-0.003	-0.000	-0.001	0.018	0.026	0.032	-0.109	-0.022	0.045	-0.198	-0.068
$\Delta\bar{\sigma}_z$	-0.118	0.031	-0.467	-0.046	0.080	0.002	0.000	0.002	0.003	0.018	-0.687	-0.113	-0.043	0.141	0.042	0.033
$\Delta\bar{\sigma}_L$	0.015	-0.017	0.481	-0.022	-0.009	0.004	-0.000	-0.000	-0.026	0.009	-0.242	-0.043	0.005	-0.097	-0.043	0.026
$\Delta\bar{\sigma}_t$	0.136	0.043	-1.525	0.068	-0.071	0.008	-0.000	-0.001	-0.033	-0.026	0.378	0.125	0.038	0.150	0.083	0.057
$\Delta\overline{(\cos\theta_f)}$	-0.018	0.003	-0.451	-0.030	0.021	0.000	-0.000	0.003	-0.015	0.012	-0.523	-0.033	-0.011	0.003	0.011	0.017
$\Delta\overline{\lvert\phi_f\rvert}$	-52.136	2.553	6.987	0.329	-5.901	-0.647	-0.026	0.931	3.493	-0.130	15.559	2.963	3.192	18.212	7.190	0.918
$\Delta s(E_g/E_i)$	-0.182	0.009	-0.186	-0.046	-0.033	-0.002	-0.000	-0.002	0.011	0.018	-0.188	-0.019	0.018	-0.034	-0.145	-0.038
$\Delta s(\sigma_z)$	0.013	-0.004	-0.114	-0.002	-0.030	0.002	-0.000	-0.002	0.004	0.000	0.487	0.041	0.016	0.127	-0.023	-0.023
$\Delta s(\sigma_L)$	-0.013	-0.005	-0.538	-0.021	0.046	0.001	-0.000	0.001	0.020	0.008	0.413	0.007	-0.024	0.059	-0.081	-0.016
$\Delta s(\sigma_t)$	-0.134	0.008	0.489	0.022	-0.083	-0.010	-0.000	-0.015	0.077	-0.009	0.251	0.015	0.044	-0.502	-0.181	-0.080
$\Delta s(\cos\theta_f)$	0.001	0.000	0.012	0.002	-0.018	0.002	0.000	-0.002	0.004	-0.000	0.344	0.018	0.010	0.088	0.004	-0.011
$\Delta s(\phi_f)$	6.473	2.584	-135.163	0.354	1.317	1.136	-0.009	-0.058	1.319	-0.140	-24.577	3.889	-0.712	-19.366	1.121	0.390
Mean Input Level $(\bar{x}_j)$		1.152	1.375	-4.83	1.732	142.5	142.5	22.5	1.151	1.151	1.375	-4.83	-4.83	1.035	1.725	1.725
Exponent (n_j)		1	1	1	1	1	2	1	1	2	1	1	2	1	1	2

Notes:

1. Correlated differences (ΔY_i) are positive when adsorbed contaminant or lattice temperature decreases correlated quantity (Y_i).
2. Tabulated values are the correlation coefficients in the following relationship:

$$\Delta Y_i = \bar{Y}_i + \sum_{j=1}^{15} A_{ij}(x_j - \bar{x}_j)^{n_j}$$

3. These coefficients are only indicative of relative importance, because they have been calculated with a relatively small factorial design.

only a monolayer of adsorbate. As pointed out by Cook (Ref. 15), oxygen will be the most persistent adsorbate in most situations, and the consideration of interaction with an oxygen layer is an important specific application to be considered in future work.

The results of calculations using the adsorbed layer model is discussed in the section on parametric analysis, where the dominance of the surface layer is clearly shown in the energy exchange correlations.

LATTICE THERMAL MOTION

There were two major difficulties that prevented including thermal motion in the original theory of Ref. 1. The first is that the conservation of total energy, which is a vital monitor on the accuracy of each trajectory computation, would not be preserved because the statistics would not be reliable in the small sample of lattice atoms (a few hundred at most). The second was that the introduction of randomness and the presence of another independent variable would be seriously detrimental to the number of runs required to achieve a certain level of confidence in the results. Completion of the statistical plan of Ref. 2 and the achievement of a moderately reliable correlation for energy exchange established a good standard of reference that greatly relieved the second difficulty. The first difficulty was overcome by choosing an approximate model for the thermal motion that should represent the major effects correctly, but still preserves a reliable energy balance for any number of lattice atoms.

An arbitrary vibrational energy per lattice atom was assigned as an input variable. Complete equipartition was then enforced; i.e., each lattice atom has the same vibrational energy in each of the three orthogonal directions (x, y, z). This determined the vibrational amplitudes, after which a random number generator assigned arbitrary initial phase angles to each of the three directions for each atom. From that point the integration of the motion of each oscillator subject to the forces of the gas particle (and in the case of the coupled oscillator lattice, the nearest neighbors) proceeded in the usual way. Because the exact quantity of energy originally possessed by each atom was known, it was a simple matter to take it into account in the energy balance. A more realistic distribution of initial lattice states would make this process considerably more difficult.

In the present model one defines an effective temperature such that the total energy of each atom (6 degrees of freedom) is $3kT_w$. Figures 4, 5, and 6 show a few early results of varying $E_w \equiv 3kT_w/E_i$ with all other input variables fixed. The centroid of the experimental region of the 64-run plan of Ref. 2 was chosen to determine "typical" values for all of these other variables. These results should not be interpreted as being more than an indication of probable wall temperature effects, because they cannot show the coupling with other input parameters (most notably the natural frequency-collision duration variable, $\omega_n\tau_c$), and because there are not enough cases to properly average out the randomness inherent in the lattice motion.

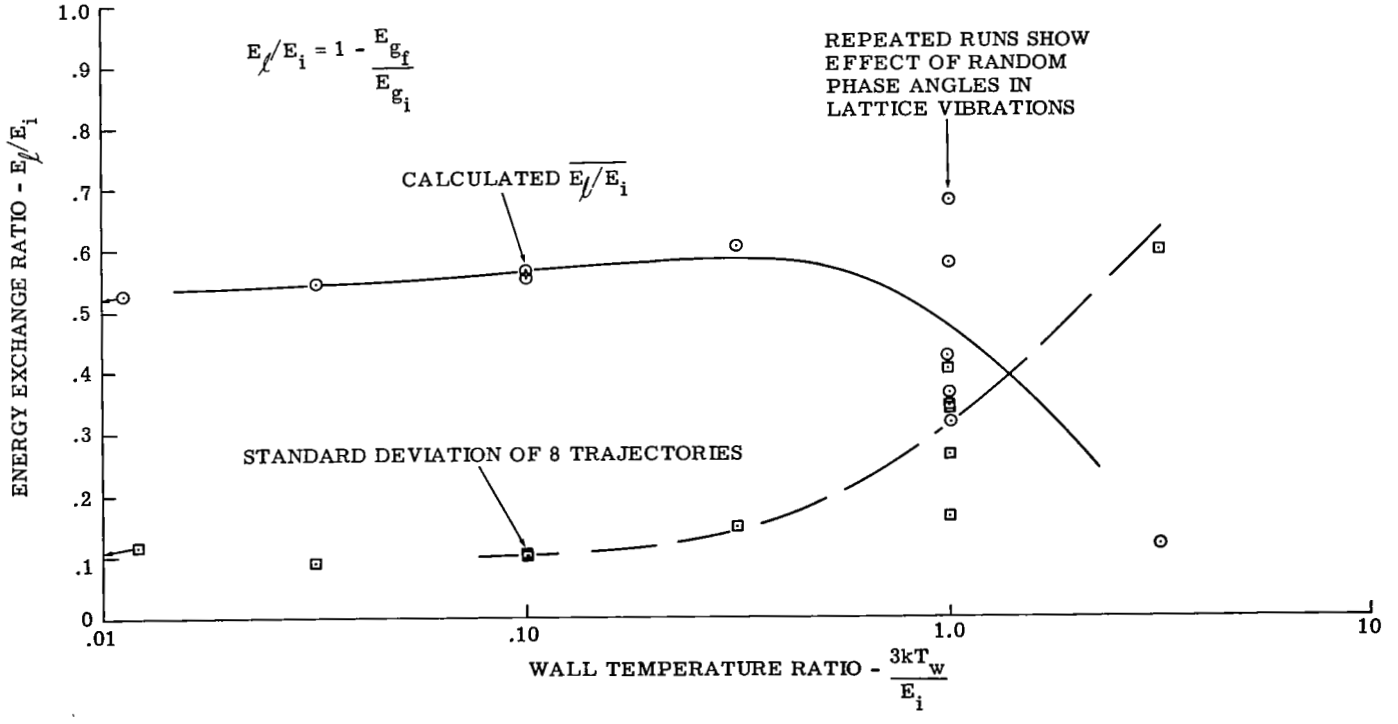

Fig. 4 Wall Temperature Effect on Energy Exchange at Center of Experimental Region

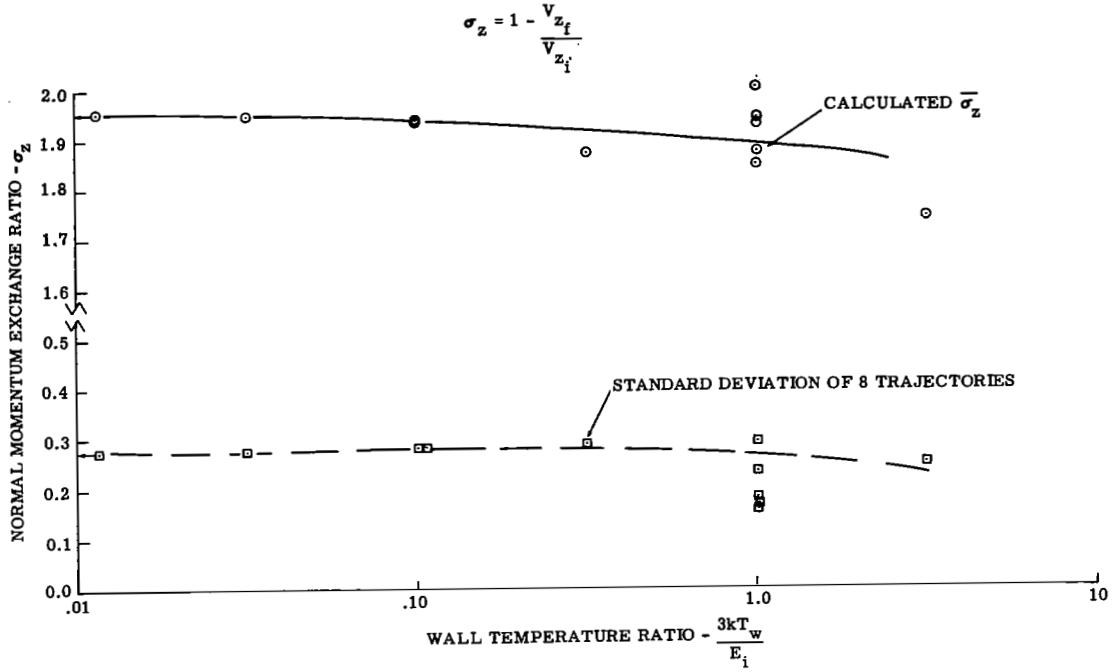

Fig. 5 Wall Temperature Effect on Normal Momentum Exchange at Center of Experimental Region

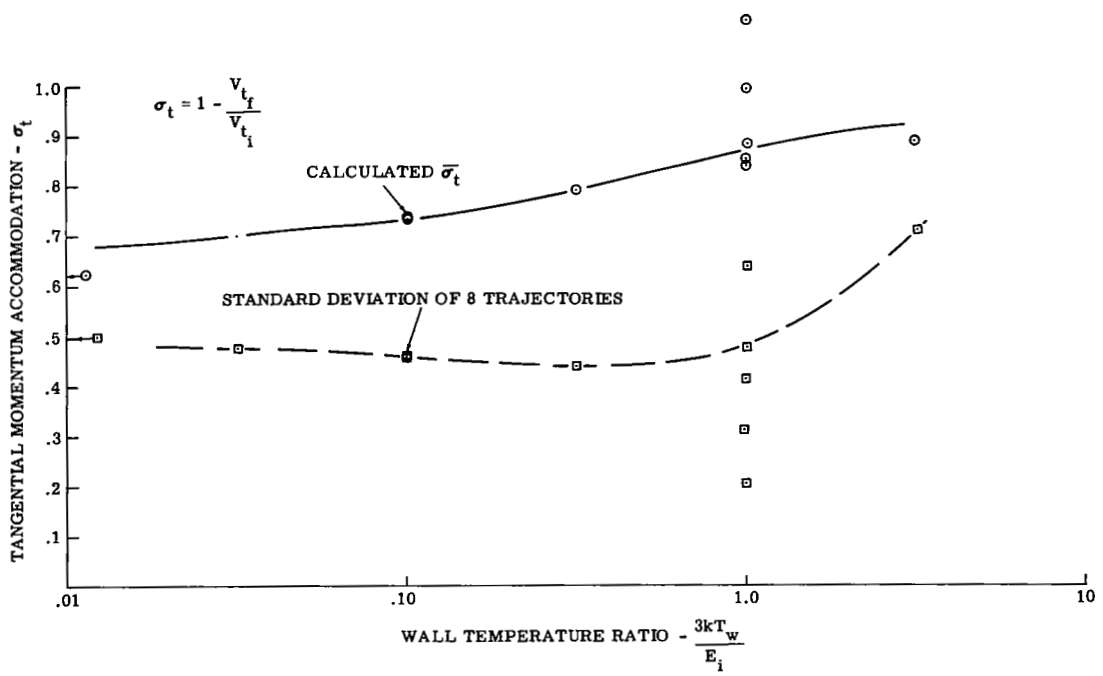

Fig. 6 Wall Temperature Effect on Tangential Momentum Accommodation at Center of Experimental Region

PARAMETRIC ANALYSIS

The large number of independent variables necessary to determine the state of a gas-surface interaction, and the relatively restricted availability of high speed computation on the required scale demand that final results of the investigations be correlated in a form which can readily be evaluated. The use of nondimensional parameters caused the number of independent variables for the simplest case (monatomic gas, no thermal motion or surface contamination, specified lattice structure) to be reduced from eight to six. Two well-established analytical techniques, statistical analysis and similitude, were used. The former approach was employed extensively in Ref. 2, and is also employed in the current effort to analyze the effects of wall temperature and adsorbed surface layers. This section describes efforts to exploit a highly simplified model of the energy exchange process in a gas-surface interaction by correlating the results of the trajectory calculations in the mathematical forms suggested by the simpler model. The first effort along these lines was described in Ref. 1, but the present approach has proven far superior to that analysis. The assumptions and form of the following analysis rest heavily on qualitative experience from a large number of calculated trajectories, and on trial and error for several correlation forms, as well as on the indicated mathematical development.

The energy exchange in the primary encounter with the lattice is assumed to take place exclusively with a single atom. This impact atom responds to the force field of the passing gas particle and accepts a predictable fraction of the gas particle's energy, after which this model assumes that the lattice atom persists in steady state oscillation. In an actual lattice, the energy accepted would be propagated rapidly to neighboring atoms. Following this encounter, the gas particle must either retain sufficient momentum normal to the surface to "climb out" of the long range attractive potential well of the entire crystal, or be pulled back to encounter another surface atom. Each subsequent collision reduces the possibility of escape, therefore we assume that a second surface collision results in complete accommodation.

Primary Collision

The driving force acting on the lattice atom in terms of an assumed time dependence, is characterized by

$$F(t) = F_o g(t, a) \tag{1}$$

where F_o and a are parameters to be determined from input conditions and the correlation of the results of the large scale numerical computations of Ref. 2. Specific forms that have been tried for $g(t, a)$ are indicated in Table III. The lattice is at rest at $t = -\infty$.

The assumption of a particular time dependence carries with it the need for a consistent method of characterizing the amplitude and duration of the force pulse. In the first attempt at a parametric analysis of the problem (Ref. 1), a simplified momentum balance was employed to determine an effective distance of closest approach between lattice atom and gas particle. Although conceptually consistent, the steepness of the intermolecular potential made this approach much too sensitive to changes of input conditions, and the resulting expressions for the force amplitude were not too useful. An approach that is related to the previous one, but which gives a better behaved expression, follows.

In the hard sphere limit (HSL), where the duration of contact is so short that lattice displacement during contact can be neglected, the energy of the lattice atom immediately following impact is all kinetic and given by the well-known formula*

$$E_\ell = \begin{cases} \dfrac{4\mu}{(1+\mu)^2} E_i & \mu \geq 1 \\ E_i & \mu < 1 \end{cases} \tag{2}$$

*All further discussion treats $\mu \geq 1$. The alternate case is treated as in Eq. (2).

TABLE III

ASSUMED FORCE-PULSE SHAPES AND

RESULTING ENERGY EXCHANGES — PRIMARY COLLISION

	$F(t)/F_o$	$\frac{(1+\mu)^2}{4\mu}\alpha$
1. Sine Pulse	$0 \quad t \leq 0$ $\sin$ at $0 < t \leq \frac{\pi}{a}$ $0 \quad t > \frac{\pi}{a}$	$\frac{\pi^4}{2} \frac{1 + \cos \frac{\pi\omega_n}{a}}{\left[\left(\frac{\pi\omega_n}{a}\right)^2 - \pi^2\right]^2}$
2. Triangular Pulse	$0 \quad t \leq 0$ $\frac{2t}{a} \quad 0 < t < a/2$ $\frac{2(a-t)}{a} \quad a/2 < t < a$ $0 \quad t \geq a$	$\frac{16}{\left(\frac{\pi\omega_n}{a}\right)^4} \left[6 + 2\cos\frac{\pi\omega_n}{a} - 8\cos\frac{\pi\omega_n}{2a}\right]$
3. Absolute Exponential Pulse	$\exp\left\{-a\lvert t\rvert\right\}$	$\frac{a^2}{a^2 + \omega_n^2}$
4. Gaussian Pulse	$\exp\left\{-at^2\right\}$	$\exp\left\{-\frac{\omega_n^2}{2a}\right\}$

Similarly, the momentum is

$$p_\ell = \sqrt{2m_\ell E_\ell} = \frac{2\mu}{1+\mu} p_i \qquad (3)$$

where μ is the mass of the lattice atom divided by that of the gas particle [note that this is the reciprocal of the μ used by Goodman (Ref. 16) and Cook (Ref. 15)] and subscripts ℓ and i denote lattice and incident quantities, respectively.

Figure 7 shows the results of several trajectory calculations conducted specifically to assess the validity of applying the HSL to the model. All of these cases have very low natural frequencies (soft springs) in the lattice, and are of normal incidence. They demonstrate the effect of the momentum constraint in Eq. (2), even when the collision partners have "soft" potentials and a significant lattice structure.

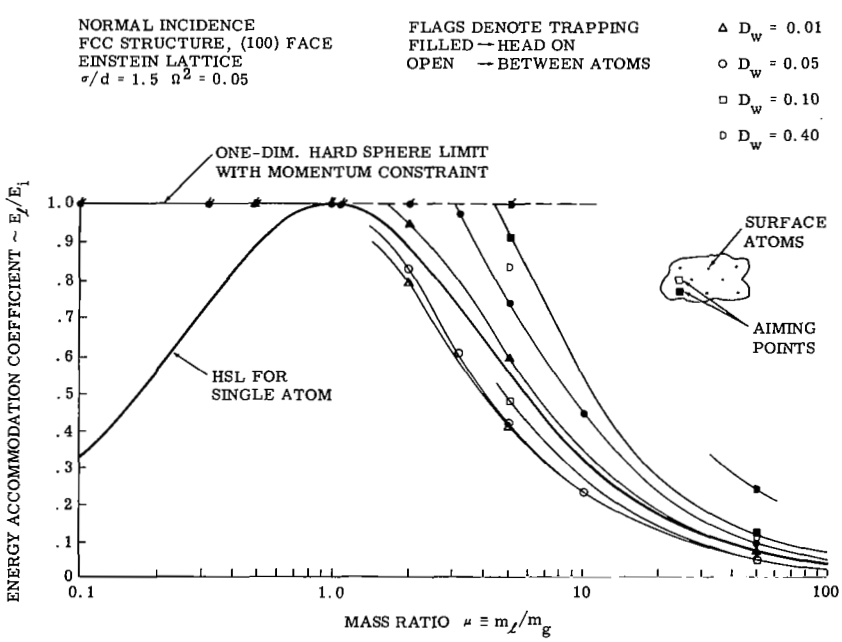

Fig. 7 Energy Accommodation Coefficient as a Function of Mass Ratio

In an elastic collision between "soft" spheres, the expression for the final lattice momentum is given by

$$p_\ell = \int F(t)\ dt \tag{4}$$

if the forces of the springs are neglected. It is assumed that the impulse transmitted to a lattice atom with springs is the same as in the "hard" sphere limit, namely,

$$\int F(t)\ dt \cong \frac{2\mu}{1+\mu}\, p_i \tag{5}$$

When the integration of Eq. (5) is carried out for each of the pulse shapes given in Table III, and the equation of motion for the forced harmonic oscillator is solved for the final total oscillator energy in each case, the expressions given in Table III for the final lattice energy ratio result. Clearly, each case reduces to the correct form in the HSL, and each shows a vanishing accommodation as ω_n (the natural angular frequency of the lattice) approaches infinity. The above assumptions, therefore, have the effect of decoupling the inertial factor from the dynamic response factor associated with the spring. In each of the four cases the result is a one parameter expression for the energy accommodation in the primary collision.

At this point in the development empirical criteria are introduced. Analysis of the results of the 83 separate cases first reported in Ref. 2 showed that the best fit over the complete dynamic range could be achieved by use of the Gaussian pulse, case 4 in Table III. The interesting feature at this stage is that the value of "a" that gives the best fit to the data is very close to $50(V_i/\sigma)^2$, where V_i is the incident molecular velocity and σ is the LJ 6-12 molecular diameter. The characteristic collision time is, therefore, very much less than that expected from simple physical reasoning.

Geometric Correction

The traditional hard sphere mass law assumes a head-on collision of the gas particle with the impact atom. In a glancing collision, the logical extension of this relationship would be

$E_\ell/E_i = \frac{4\mu}{(1+\mu)^2} \cos^2\theta_R$, where θ_R is the angle between the incident direction and the recoil direction. In an actual case in which incident trajectories are uniformly distributed over the cell surface structure, the effective mean for the recoil angle becomes very difficult to determine. The numerical results agree very well with

$$\alpha = -\alpha_{\text{head-on}} (\cos\theta_i) \tag{6}$$

where θ_i is the angle between the incident velocity and the surface normal. The modification implied by Eq. (6) is applied to the results for the head-on primary collision to give

$$\alpha_p = -\frac{4\mu\cos\theta_i}{(1+\mu)^2} e^{-a'\left(\frac{\omega_n\sigma}{V_i}\right)^2} \tag{7}$$

where the present best value for a' is ~ 0.011.

Long Range Effects

Although the assumption that a single lattice atom dominates the energy exchange has been well supported by experience in a large number of cases, the effects of long range forces from the entire crystal are still significant, particularly at lower incident energies. These effects arise in two ways. First, the incident particle falls through a potential well before striking the impact atom, and therefore has an increased effective incident energy. Although this energy must be "paid back" in "climbing away" from the lattice, the gas energy at that point has been reduced by the primary collision. This effect can be accounted for by the following correction:

$$(E_i)_{z_o} = (E_i)_\infty + A(E_i)_\infty \tag{8}$$

where A is the normalized attractive potential at the approximate location of the primary collision. The corrected accommodation coefficient then becomes

$$\frac{E_\ell}{E_{i_\infty}} = \frac{E_\ell}{(E_i)_{z_o}} (1 + A) \tag{9}$$

If the point centers of potential are assumed to be continuously distributed in a semi-infinite lattice, the total attractive potential on a particle at z_o can be found, by a spherical integration, to be

$$\Phi = \frac{2\pi}{3} n \left(\frac{\sigma}{z_o}\right)^3 (\sigma/d)^3 \epsilon \tag{10}$$

where d is the lattice grid spacing parameter (1/2 unit cell edge for FCC and BCC, one unit cell edge for simple cubic, and 1/5 the edge for diamond structure), n is the number of lattice atoms per volume of d^3, and ϵ is the Lennard-Jones 6-12 binding energy. E_i will hereinafter be considered as being established as $z \to \infty$. For present purposes it is assumed that $z_o \approx \sigma$, a value which represents trajectory experience fairly well, and

$$A = \frac{2\pi n}{3} \left(\frac{\sigma}{d}\right)^3 \frac{\epsilon}{E_i \cos^2\theta_i} \tag{11}$$

*

where the $\cos^2\theta_i$ term accounts for incident angles other than normal, as it is only the energy equivalent of the normal momentum that is involved with the attractive potential in the continuum approximation.

The second and most important way in which the long range forces affect the interaction is in the trapping of portions of the true exiting distribution of molecules. There is no rational approach to modeling this effect in the absence of a good description of the output distributions as a function of input conditions. The experience provided by the 83 cases for which there are numerical calculations of 18-unit samples of the output distributions again supply the needed criteria. The mean exit normal momentum

---

*See also Eq. (11a) for treatment in the case of adsorbed surface contaminants.

for a given incident state depends strongly on the incident normal momentum, the energy exchange in the primary encounter, and the lattice surface configuration. The practice adopted here has been to express that fraction of the exit distribution of states which has insufficient normal momentum to prevent trapping as an empirically determined function of the incident normal momentum.

This relationship is expressed as

$$\frac{\bar{p}_z^2}{2m_g} \equiv b \cos^2\theta_i (1 + A)(1 - \alpha_p)(1 - e^{-1/A}) \tag{12}$$

where again the best value for b has been determined from analysis of the numerical data to be very close to 1/2, and $\bar{p}_z$ is the ratio of mean exit normal momentum to the incident normal momentum. The last factor in Eq. (12) has been introduced somewhat arbitrarily to enforce complete trapping in the limit of small incident energy. It has very little effect on cases having high incident energy.

Whenever $\bar{p}_z^2 < 2m_g A$, some portion of the exit distribution will experience additional collisions with the lattice and be trapped or adsorbed. An effective trapped fraction η can be estimated for these cases by

$$\eta = 1 - \frac{\bar{p}_z^2}{2m_g A} \tag{13}$$

Because trapping results in complete accommodation, the resulting final expression for correlating the numerical data for cold surfaces becomes

$$\alpha = (\eta - 1)\cos\theta_i \left[\frac{4\mu(1 + A)}{(1 + \mu)^2}\right] e^{-a'\left(\frac{\omega_n \sigma}{V_i}\right)^2} + \eta \tag{14}$$

This relationship was used to generate the correlation in Fig. 8.

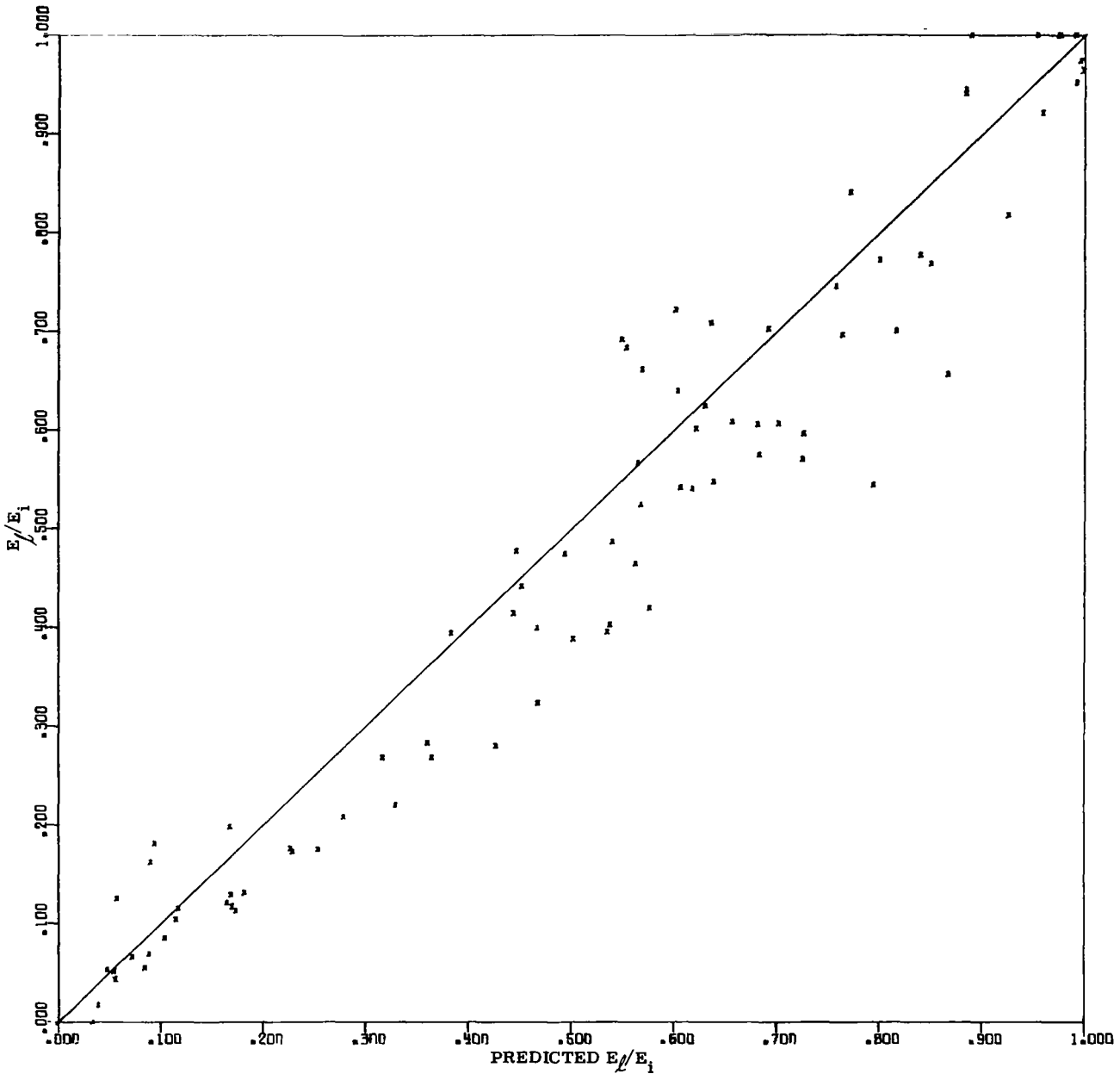

Fig. 8 Correlation by Eq. (14) of 83 Cases from Ref. 2

Correlation of Wall Temperature Effects

In order to perform any comparison between the results and existing data, there must be some understanding of the effects of lattice thermal motion. Although a crude model for treating this case is available in the trajectory calculations, an extension to the parametric analysis to account for thermal motion is also required.

Marsh (Ref. 17) suggested a relaxation model for gas-surface interactions. Although this analysis does not use his model, the same concept of a relaxation toward thermal equilibrium during the time of residence has been employed. The conventional definition of thermal accommodation coefficient is avoided here, because it has singularities for cases in which the distribution of incident energies is non-Maxwellian (cf., Goodman, Ref. 18). Logan and Stickney (Ref. 19) present an alternate thermal model which shows promising agreement with thermal effects in molecular beam scattering, but a simpler relationship is sufficient for present purposes.

The exiting gas particle energy is assumed to be at least as large as that resulting from interaction with the same lattice in a cold condition. The correlation equation [Eq. (14)] is employed to define this condition. If permitted to remain in contact with the lattice for an indefinite period, the gas particle would emerge with an average energy $\frac{n+1}{2} kT_w$, where n is the number of active degrees of freedom of the gas particle. This energy is therefore assigned to all particles trapped [i.e., the fraction η in Eq. (14)]. After a primary collision the gas-particle energy will probably be increased by lattice thermal vibrations, and that the amount of this increase should depend on the time (measured in lattice vibration cycles) that the incident particle spends in the vicinity of the lattice. The following equation quantizes this argument:

$$E_\ell(T_w) = E_\ell(0) - \eta \frac{n+1}{2} kT_w - (1-\eta)\left(\frac{n+1}{2} kT_w\right)\left(1 - e^{-c \frac{\omega_n \sigma}{V_i}}\right) \qquad (15)$$

Once again curve fitting is used to determine a best value for the relaxation constant c. The present best value for c appears to be about 0.2.

Although the results of employing Eq. (15) to correlate cases having large values of $3kT_w/E_i$ show a lot of scatter, the approach appears to be adequate for the present purposes. The observed correlation errors seem to be almost completely due to the small sample of random phase angles in the individual encounters, and at this writing, there appears to be no significant effect of any other physical variable on the correlation. Figure 9 shows results of 70 cases involving different lattice structures, wall temperatures, and adsorbed species configurations correlated against Eq. (15). The input data and the other results of these runs are tabulated in the Appendix. The adsorbed contaminant properties were used in evaluating Eq. (15). The only effect of the bulk that was included was in computing the long-range attractive force, for which Eq. (11) was modified to superpose the bulk and surface-layer attractions. Because the bulk is one lattice-point spacing further away, Eq. (11) becomes in this case

$$A = \frac{2\pi n}{3E_i \cos^2\theta_i}\left[\epsilon_s\left(\frac{\sigma}{d}\right)_s^3 + (\epsilon_b - \epsilon_s)\frac{\left(\frac{\sigma}{d}\right)_b^6}{\left(1 + \frac{\sigma}{d}\right)_b^3}\right] \qquad (11a)$$

where the subscripts b and s denote bulk and surface properties, respectively. This change is important when the attraction of the bulk is very much greater than that of the surface.

Determination of Empirical Parameters

Numerical values for the coefficients a, b, and c which have been introduced to account for factors that cannot be rationally evaluated in the model, have been determined by iteration in order to minimize the differences between values predicted for α by Eq. (15) and the values resulting from the numerical trajectory calculations of Ref. 5. The error measurement that was finally chosen for minimization (several others were also tried) was

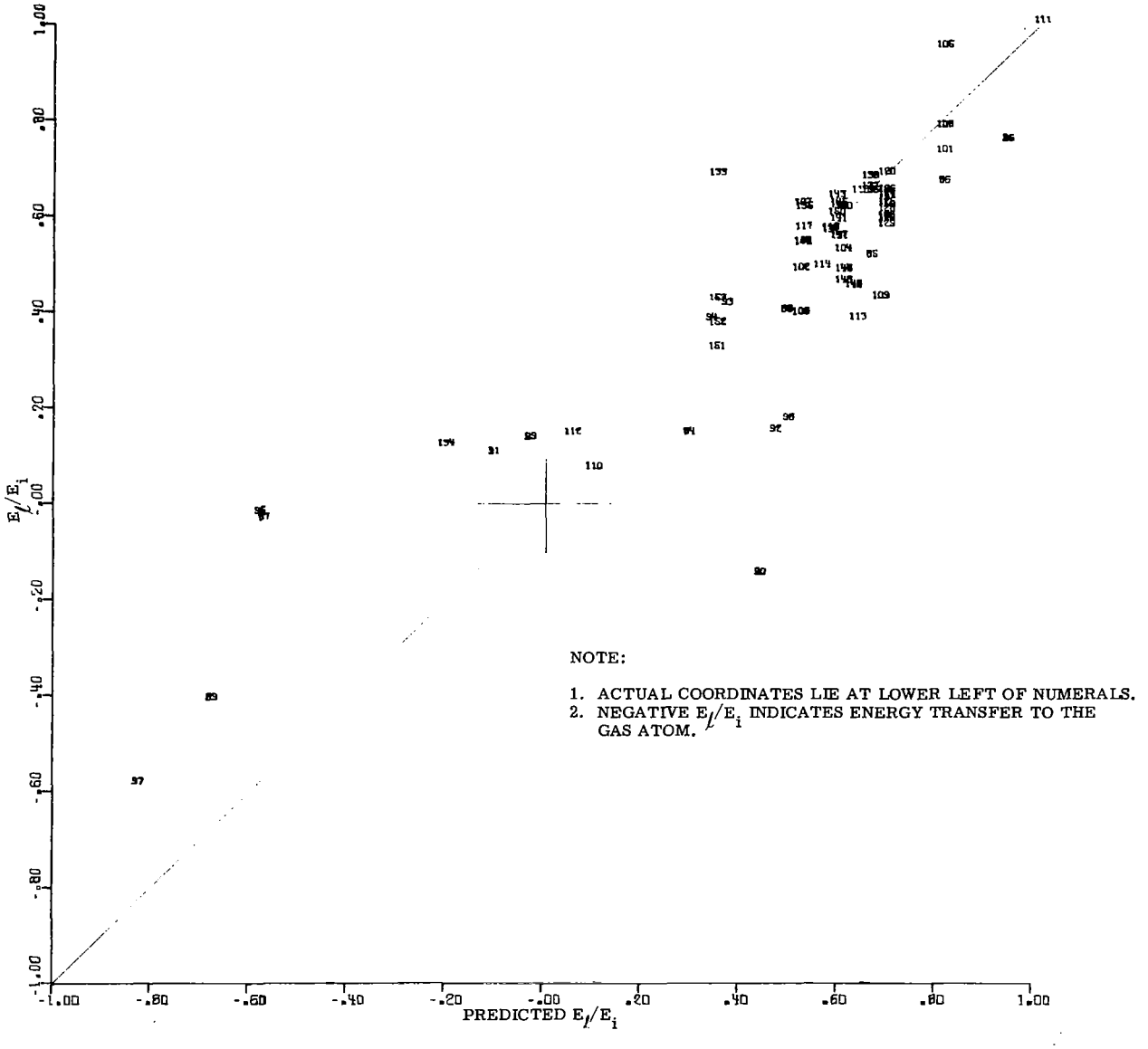

Fig. 9 Correlation by Eq. (15) of 70 Runs Involving Wall Temperature, Surface Structure, and Adsorbed Monolayers

$$\delta = \frac{1}{N} \sum_{n=1}^{N} \frac{|\alpha_{calc} - \alpha_{pred}|}{0.05 + \frac{1}{2}(\alpha_{calc} + \alpha_{pred})} \qquad (16)$$

The form of Eq. (16) was employed to give roughly equal weight to the cases having high and low values of α, to avoid accidental zeros in the denominator, and to prevent one or two very large differences from disproportionately affecting the optimization. The resulting values for several statistical measures of the degree of correlation are given in Table IV, and the correlations are displayed graphically in Figs. 8 and 9. It is important to realize that the indicated data are distributed over wide ranges of the input data, namely:

$$0.32 \leq \frac{\omega_n d}{V_i} \leq 10 \qquad 0.001 \leq \frac{\epsilon}{E_i} \leq 0.577$$

$$1.25 \leq \sigma/d \leq 1.9 \qquad 1.47 \leq \mu \leq 14.7$$

$$120° \leq \theta_i \leq 165° \qquad \phi_i = 15°,\ 30°$$

TABLE IV

STATISTICAL RESULTS OF CORRELATION (EQ. 15)

$a' = 0.01089$ $\quad b = 0.531$ $\quad c = 0.2$

	83 Cases of Fig. 8 (from Ref. 5)	70 Cases of Fig. 9
δ [From Eq. (16)]	0.17	0.58
Standard Error $\sqrt{\frac{\Sigma(\Delta\alpha)^2}{N}}$	0.09	0.18
Average Error $\frac{\Sigma\lvert\Delta\alpha\rvert}{N}$	0.068	0.12

Aside from the obvious benefits of a closed algebraic expression for the energy accommodation, the present form has heuristic benefits associated with the clear distinction between the various mechanisms in the over-all process. The best demonstration

of this is shown by the effective collision time for the present group of interactions, which turns out to be an order of magnitude less than that expected from molecular diameter and incident velocity [see Eq. (7)]. This result helps explain why the independent-oscillator lattice (IOL) model differs so little from the coupled-oscillator model (COL) in the cases investigated in Ref. 2. One would expect that the IOL would be an acceptable approximation only if $\omega_n \tau_c < 1$, where τ_c is the effective collision time. In Ref. 2, τ_c was calculated by an expression which was not very different from σ/V_i, and reasonably small differences between IOL and COL were found when $\omega_n \tau_c$ had a value as great as 40. This fortunate result could not be explained until the present analysis showed that a more correct value for τ_c is about $0.15\ \sigma/V_i$. This, coupled with the inherent decrease in energy exchange in all lattice models as $\omega_n \tau_c$ increases, yields a maximum difference between models in energy exchanged at around $\omega_n \sigma/V_i = 10$. Insights of this type should prove in the long run to be the greatest benefit of the present approach.

CONCLUSIONS

Numerical calculation of gas-surface interactions is now producing results of apparent practical value. The bulk of the work remaining is concerned with the resolution of complicating phenomena and corrections for shortcomings in the models. The need for experimental data on well-characterized surfaces in the appropriate energy range is more urgent than ever, because one still cannot be sure of the physical reality of any part of this approach until it has been carefully tested. Both scattered flux distributions and energy exchange data are required, as these phenomena are clearly not connected in any unique way. The major trends shown in these theoretical results should also be present in good experimental results, but it is probably not realistic to expect a very high quantitative accuracy for any specific case.

To briefly summarize the most important results of this report:

1. Lattice configuration and azimuth angle of incidence have been shown to be of minor importance to the gross properties of

reflected distributions, except for very rough crystal planes such as FCC (110) where the geometric effect is only moderate.

2. A relatively simple correlation equation, derived from a highly idealized interaction model, gives a prediction of energy exchanged with the lattice from known incident conditions. The prediction accuracy, when measured against the computed cases that are presently available, appears quite adequate in view of the uncertainties in the computed cases themselves. The correlation includes effects of finite lattice temperature, and can handle adsorbed contaminants if their physical characteristics are known.

3. Adsorbed contaminants, insofar as the present model reflects their real characteristics, will almost always control the energy and momentum exchanges in gas-surface interactions. Even a monolayer will almost completely isolate the gas particle from the influence of the bulk. Knowledge of the surface structure and bonding characteristics of such layers is therefore of first-order importance.

4. A crude model of the thermal statistics of a "warm" lattice showed no important effects on gross properties of the interactions until the thermal energy per lattice atom became comparable to the incident energy of the gas particle. Although not of any real importance to hypervelocity flight, these lattice thermal effects will play an important role in attempts to employ thermal cell data for checking predictions of energy accommodation.

5. Statistical correlations of the data from a small pattern of cases designed to display wall temperature and surface contaminant effects are given. Although these data complement the correlation equation for energy exchange, their primary value lies in their characterization of momentum and spatial flux distributions as a function of incident conditions. The results are compared against previously published corresponding cases for cold, clean surfaces (Refs. 2 and 20).

6. The force pulse shapes that give best correlation with calculated energy exchange are much more sharply peaked than was originally expected from simple physical arguments. This fact appears to explain why the independent-oscillator model works as often as it does. The portion of the collision interval during which significant energy is exchanged is usually small relative to the time required for propagation of energy from one lattice atom to another in a real lattice, even at incident energies less than one ev.

APPENDIX

TABULATION OF RESULTS

The following pages contain data from the cases described in the text. The first 64 cases are available in greater detail in Ref. 20. The mean values and standard deviations of the output parameters for all 153 cases run to date are presented along with the corresponding input variables. The aiming point pattern for runs 1-83 is a 7 x 7 point rectangular grid on the surface of the FCC unit cell, giving 18 unique trajectories. Runs 84-153 use a 5 x 5 point rectangular grid on the surface projection of a unit cell. This pattern yields 8 unique trajectories for the FCC, DC, HCP, and BCC (110) structures, and 16 for SC and BCC (100).

The format shown below is employed for data presentation. The first two rows contain input data and the third and fourth rows contain the mean and standard deviation, respectively, of the output parameter. Means are denoted by bars, and standard deviation values of x by $S(x)$. Symbols are defined in the report, except for the code FC, which is as follows:

FC	-1	0	2	3	4	5	6	7
Lattice Configuration	BCC (100)	SC (100)	DC (100)	FCC (111)	FCC (110)	FCC (100)	BCC (110)	HCP (100)

The over-all data format is:

Run No.	Ω_s^2	θ_i	ϕ_i	σ_s/d	ϵ_s/E_i	$e^{-a'\left(\frac{\omega_n \sigma}{V_i}\right)^2}$	Predicted $\overline{E_\ell/E_i}$
	μ_s	Ω_B^2	μ_B	FC	σ_B/d	ϵ_b/E_i	E_w/E_i
	$\overline{E_g/E_i}$	$\overline{V}$	$\overline{\sigma_z}$	$\overline{\sigma_L}$	$\overline{\sigma_t}$	$\overline{\cos\ \theta_f}$	$\overline{\lvert\phi_f\rvert}$
	$S(E_g/E_i)$	$S(V)$	$S(\sigma_z)$	$S(\sigma_L)$	$S(\sigma_t)$	$S(\cos\ \theta_f)$	$S(\phi_f)$
1	0.1000	120.0000	60.0000	1.2500	0.0010	0.9983	0.4473
	2.0000	0.1000	2.0000	5.0000	1.2500	0.0010	0.
	0.5227	0.7094	2.1882	-0.0955	0.4517	0.5941	33.7400
	0.1918	0.1396	0.4620	0.2220	0.3146	0.2313	33.6000
2	10.0000	150.0000	75.0000	1.2500	0.0040	0.8421	0.6553
	2.0000	10.0000	2.0000	5.0000	1.2500	0.0040	0.
	0.3910	0.6191	1.8494	0.0076	0.7762	0.7356	35.5400
	0.1140	0.0883	0.2200	0.2557	0.6406	0.1905	110.7600
3	1.0000	165.0000	75.0000	1.5000	0.0010	0.9756	0.8408
	2.0000	1.0000	2.0000	5.0000	1.5000	0.0010	0.
	0.2226	0.4654	1.8205	0.0006	0.7427	0.7925	26.2400
	0.0723	0.0781	0.1760	0.2046	0.7781	0.1701	113.2600
4	100.0000	135.0000	60.0000	1.5000	0.0040	0.0842	0.0544
	2.0000	100.0000	2.0000	5.0000	1.5000	0.0040	0.
	0.9570	0.9782	2.0551	-0.0454	0.4100	0.7460	23.3600
	0.0294	0.0151	0.2960	0.3117	0.4801	0.2093	68.6800
5	0.1000	135.0000	75.0000	1.5000	0.0160	0.9975	0.5025
	4.0000	0.1000	4.0000	5.0000	1.5000	0.0160	0.
	0.6113	0.7792	1.8671	-0.0285	0.3016	0.6131	35.6500
	0.1028	0.0664	0.3623	0.2579	0.3131	0.2562	31.9800
6	10.0000	165.0000	60.0000	1.5000	0.0640	0.7808	0.5997
	4.0000	10.0000	4.0000	5.0000	1.5000	0.0640	0.
	0.2781	0.5591	1.4153	-0.0348	0.6250	0.4514	32.0920
	0.1423	0.1036	0.3785	0.3092	1.1770	0.3575	92.2950
7	1.0000	149.9999	60.0000	1.2500	0.0160	0.9830	0.5686
	4.0000	1.0000	4.0000	5.0000	1.2500	0.0160	0.
	0.4755	0.6852	1.7875	-0.0086	0.7307	0.6820	7.0750
	0.1078	0.0780	0.2390	0.3181	0.7138	0.2071	98.1290
8	100.0000	120.0000	75.0000	1.2500	0.0640	0.1793	0.0874
	4.0000	100.0000	4.0000	5.0000	1.2500	0.0640	0.
	0.8377	0.9704	2.1139	-0.0595	0.5192	0.6266	46.0680
	0.3010	0.0295	0.6332	0.4241	0.4089	0.2629	52.3010

The over-all data format is:

Run No.	Ω_s^2	θ_i	ϕ_i	σ_s/d	ϵ_s/E_i	$e^{-a'\left(\frac{\omega_n \sigma}{V_i}\right)^2}$	Predicted $\overline{E_\ell/E_i}$
	μ_s	Ω_B^2	μ_B	FC	σ_B/d	ϵ_b/E_i	E_w/E_i
	$\overline{E_g/E_i}$	$\overline{V}$	$\overline{\sigma_z}$	$\overline{\sigma_L}$	$\overline{\sigma_t}$	$\overline{\cos\ \theta_f}$	$\overline{\lvert\phi_f\rvert}$
	$S(E_g/E_i)$	$S(V)$	$S(\sigma_z)$	$S(\sigma_L)$	$S(\sigma_t)$	$S(\cos\ \theta_f)$	$S(\phi_f)$
9	0.1000	165.0000	75.0000	1.2500	0.0040	0.9983	0.6225
	4.0000	0.1000	4.0000	5.0000	1.2500	0.0040	0.
	0.3987	0.6205	1.7500	0.0044	0.7764	0.7244	50.1530
	0.1210	0.1172	0.2037	0.3155	1.1065	0.1969	100.7930
10	10.0000	135.0000	60.0000	1.2500	0.0010	0.8421	0.3826
	4.0000	10.0000	4.0000	5.0000	1.2500	0.0010	0.
	0.6051	0.7715	1.9551	-0.0470	0.8444	0.6961	49.3360
	0.1532	0.0990	0.2863	0.3327	0.7683	0.1985	88.1030
11	1.0000	120.0000	60.0000	1.5000	0.0040	0.9756	0.3298
	4.0000	1.0000	4.0000	5.0000	1.5000	0.0040	0.
	0.7792	0.8810	2.1541	-0.0529	0.2314	0.5770	21.7380
	0.0957	0.0550	0.4066	0.1645	0.2121	0.2033	15.3370
12	100.0000	149.9999	75.0000	1.5000	0.0010	0.0842	0.0469
	4.0000	100.0000	4.0000	5.0000	1.5000	0.0010	0.
	0.9464	0.9727	1.8806	-0.0302	0.7546	0.7626	48.5450
	0.0310	0.0160	0.1977	0.4041	0.8716	0.1713	95.2130
13	0.1000	149.9999	60.0000	1.5000	0.0640	0.9975	1.0000
	2.0000	0.1000	2.0000	5.0000	1.5000	0.0640	0.
	0.0362	0.4657	1.1138	0.0593	0.9136	0.5913	-0.6760
	0.0830	0.0500	0.2560	0.2499	0.2070	0.0598	45.3410
14	10.0000	120.0000	75.0000	1.5000	0.0160	0.7808	0.4255
	2.0000	10.0000	2.0000	5.0000	1.5000	0.0160	0.
	0.7196	0.8464	1.8209	-0.0417	0.1625	0.4104	34.3750
	0.1009	0.0603	0.3950	0.1918	0.1456	0.1975	15.5480
15	1.0000	135.0000	75.0000	1.2500	0.0640	0.9830	0.8855
	2.0000	1.0000	2.0000	5.0000	1.2500	0.0640	0.
	0.0551	0.4939	1.1709	0.0422	0.8952	0.5441	18.8410
	0.1082	0.0676	0.3544	0.1653	0.2290	0.2291	37.5570
16	100.0000	165.0000	60.0000	1.2500	0.0160	0.1793	0.1593
	2.0000	100.0000	2.0000	5.0000	1.2500	0.0160	0.
	0.8785	0.9370	1.7582	0.0060	0.7865	0.7324	48.8800
	0.0468	0.0251	0.1776	0.4106	1.7661	0.1716	102.9520

```
17    0.1000  120.0000   60.0000    1.5000    0.0640    0.9975    0.8918
      4.0000    0.1000    4.0000    5.0000    1.5000    0.0640    0.
     -0.       -0.       1.0000   -0.        1.0000   -0.       -0.
     -0.       -0.       -0.       -0.       -0.       -0.       -0.

18   10.0000  149.9999   75.0000    1.5000    0.0160    0.7808    0.4654
      4.0000   10.0000    4.0000    5.0000    1.5000    0.0160    0.
      0.6005    0.7721    1.8307   -0.0102    0.4006    0.7194   42.2600
      0.1032    0.0673    0.2322    0.3133    0.6087    0.2011   67.5690

19    1.0000  165.0000   75.0000    1.2500    0.0640    0.9830    0.6929
      4.0000    1.0000    4.0000    5.0000    1.2500    0.0640    0.
      0.2977    0.5762    1.4819   -0.0406    0.5977    0.5237   35.7030
      0.1328   -0.0772    0.4364    0.2937    1.1642    0.4117   92.4670

20  100.0000  135.0000   60.0000    1.2500    0.0160    0.1793    0.0864
      4.0000  100.0000    4.0000    5.0000    1.2500    0.0160    0.
      0.9307    0.9644    2.0089   -0.0536    0.6216    0.7134   21.7130
      0.0444    0.0231    0.2688    0.3865    0.6431    0.1901   87.6320

21    0.1000  135.0000   75.0000    1.2500    0.0040    0.9983    0.6377
      2.0000    0.1000    2.0000    5.0000    1.2500    0.0040    0.
      0.2918    0.5567    1.8831   -0.0659    0.6740    0.7025   38.7377
      0.1753    0.1357    0.4237    0.2251    0.3516    0.2148   67.6007

22   10.0000  165.0000   60.0000    1.2500    0.0010    0.8421    0.7246
      2.0000   10.0000    2.0000    5.0000    1.2500    0.0010    0.
      0.4030    0.6424    1.8013    0.0554    1.0180    0.8196   -0.5042
      0.1868    0.1192    0.2663    0.2430    0.9141    0.1810  120.9627

23    1.0000  150.0000   60.0000    1.5000    0.0040    0.9756    0.7651
      2.0000    1.0000    2.0000    5.0000    1.5000    0.0040    0.
      0.3034    0.5404    1.8391   -0.0124    0.5453    0.7267   23.9723
      0.1146    0.1068    0.2197    0.2160    0.4555    0.1904   72.1194

24  100.0000  120.0000   75.0000    1.5000    0.0010    0.0842    0.0379
      2.0000  100.0000    2.0000    5.0000    1.5000    0.0010    0.
      0.9821    0.9910    2.2067   -0.1052    0.2119    0.6034   41.2059
      0.0156    0.0079    0.3732    0.2811    0.2224    0.1866   25.0959

25    0.1000  165.0000   75.0000    1.5000    0.0160    0.9975    0.9266
      2.0000    0.1000    2.0000    5.0000    1.5000    0.0160    0.
      0.1825    0.4178    1.5266    0.0021    0.5024    0.5087   44.8013
      0.0917    0.1121    0.2877    0.2238    0.8584    0.2780   85.2093

26   10.0000  135.0000   60.0000    1.5000    0.0640    0.7808    0.8821
      2.0000   10.0000    2.0000    5.0000    1.5000    0.0640    0.
      0.0591    0.4039    1.0671    0.0093    0.8634    0.1423   17.2548
      0.1090    0.1303    0.6983    0.1489    0.2188    0.8473   27.1620

27    1.0000  120.0000   60.0000    1.2500    0.0160    0.9830    0.4941
      2.0000    1.0000    2.0000    5.0000    1.2500    0.0160    0.
      0.5252    0.7133    1.9912   -0.0705    0.3653    0.4956   27.4722
      0.1755    0.1289    0.5472    0.1923    0.2570    0.2736   24.1498
```

The over-all data format is:

Run No.	Ω_s^2	θ_i	ϕ_i	σ_s/d	ϵ_s/E_i	$e^{-a'\left(\frac{\omega_n \sigma}{V_i}\right)^2}$	Predicted $\overline{E_\ell/E_i}$
	μ_s	Ω_B^2	μ_B	FC	σ_B/d	ϵ_b/E_i	E_w/E_i
	$\overline{E_g/E_i}$	$\overline{V}$	$\overline{\sigma_z}$	$\overline{\sigma_L}$	$\overline{\sigma_t}$	$\overline{\cos\ \theta_f}$	$\overline{\lvert\phi_f\rvert}$
	$S(E_g/E_i)$	$S(V)$	$S(\sigma_z)$	$S(\sigma_L)$	$S(\sigma_t)$	$S(\cos\ \theta_f)$	$S(\phi_f)$
28	100.0000	150.0000	75.0000	1.2500	0.0640	0.1793	0.1621
	2.0000	100.0000	2.0000	5.0000	1.2500	0.0640	0.
	0.8016	0.8954	1.6576	-0.0094	0.6516	0.5695	38.7792
	0.0779	0.0435	0.3780	0.4485	0.9630	0.3275	92.7295
29	0.1000	150.0000	60.0000	1.2500	0.0010	0.9983	0.5548
	4.0000	0.1000	4.0000	5.0000	1.2500	0.0010	0.
	0.3160	0.5948	1.6897	0.0160	0.7220	0.7168	10.2699
	0.2193	0.1596	0.3655	0.2408	0.5844	0.1861	90.4229
30	10.0000	120.0000	75.0000	1.2500	0.0040	0.8421	0.2783
	4.0000	10.0000	4.0000	5.0000	1.2500	0.0040	0.
	0.7911	0.8879	2.1833	-0.1172	0.3170	0.5916	44.7948
	0.0923	0.0523	0.4276	0.2860	0.2638	0.2139	29.2305
31	1.0000	135.0000	75.0000	1.5000	0.0010	0.9756	0.4446
	4.0000	1.0000	4.0000	5.0000	1.5000	0.0010	0.
	0.5853	0.7841	1.9792	-0.0743	0.5261	0.7332	48.0419
	0.1787	0.0708	0.3453	0.2912	0.3885	0.1824	53.4105
32	100.0000	165.0000	60.0000	1.5000	0.0040	0.0842	0.0528
	4.0000	100.0000	4.0000	5.0000	1.5000	0.0040	0.
	0.9487	0.9739	1.8011	-0.0033	0.6491	0.7738	52.4764
	0.0259	0.0133	0.1502	0.4202	1.6236	0.1451	96.6474
33	0.1000	135.0000	60.0000	1.2500	0.0640	0.9983	0.5700
	4.0000	0.1000	4.0000	5.0000	1.2500	0.0640	0.
	0.3382	0.6255	1.7403	0.0200	0.8214	0.6282	11.5760
	0.2052	0.1223	0.4733	0.3261	0.4132	0.2621	86.6593
34	10.0000	165.0000	75.0000	1.2500	0.0160	0.8421	0.5388
	4.0000	10.0000	4.0000	5.0000	1.2500	0.0160	0.
	0.5138	0.7151	1.7440	0.0075	0.7959	0.7186	47.7572
	0.0730	0.0507	0.1978	0.3308	1.3578	0.1912	109.5016
35	1.0000	150.0000	75.0000	1.5000	0.0640	0.9756	0.8175
	4.0000	1.0000	4.0000	5.0000	1.5000	0.0640	0.
	0.2992	0.5775	1.5368	-0.0010	0.6276	0.5230	47.6860
	0.1741	0.1367	0.4335	0.2884	0.5599	0.3580	68.1720

36	100.0000	120.0000	60.0000	1.5000	0.0160	0.0842	0.0330
	4.0000	100.0000	4.0000	5.0000	1.5000	0.0160	0.
	1.0304	1.0151	2.2421	-0.0457	0.2048	0.6211	22.0040
	0.0232	0.0115	0.4631	0.2220	0.2702	0.2316	20.3284
37	0.1000	120.0000	75.0000	1.5000	0.0040	0.9975	0.4684
	2.0000	0.1000	2.0000	5.0000	1.5000	0.0040	0.
	0.6768	0.8206	1.8954	-0.0554	0.1881	0.4477	35.5052
	0.0954	0.0588	0.2650	0.1675	0.1237	0.1325	13.9904
38	10.0000	150.0000	60.0000	1.5000	0.0010	0.7808	0.6039
	2.0000	10.0000	2.0000	5.0000	1.5000	0.0010	0.
	0.4587	0.6728	1.8857	-0.0131	0.6957	0.7671	10.2383
	0.1050	0.0778	0.2024	0.2703	0.6025	0.1753	96.6654
39	1.0000	165.0000	60.0000	1.2500	0.0040	0.9830	0.8514
	2.0000	1.0000	2.0000	5.0000	1.2500	0.0040	0.
	0.2317	0.4615	1.8048	0.0049	0.9297	0.7774	66.7226
	0.1386	0.1370	0.2330	0.2130	0.7418	0.2251	107.6409
40	100.0000	135.0000	75.0000	1.2500	0.0010	0.1793	0.1132
	2.0000	100.0000	2.0000	5.0000	1.2500	0.0010	0.
	0.8844	0.9399	1.9558	-0.0305	0.8195	0.6759	22.9274
	0.0605	0.0323	0.2748	0.4208	0.7230	0.1944	96.4432
41	0.1000	150.0000	75.0000	1.2500	0.0160	0.9983	0.8020
	2.0000	0.1000	2.0000	5.0000	1.2500	0.0160	0.
	0.2274	0.4600	1.6192	-0.0088	0.6927	0.5363	67.6818
	0.1186	0.1286	0.3217	0.2340	0.5497	0.2787	87.7986
42	10.0000	120.0000	60.0000	1.2500	0.0640	0.8421	0.7711
	2.0000	10.0000	2.0000	5.0000	1.2500	0.0640	0.
	0.1598	0.5749	1.3348	-0.0702	0.7646	0.3767	26.6448
	0.2128	0.1763	0.5358	0.1917	0.2994	0.2875	28.5728
43	1.0000	135.0000	60.0000	1.5000	0.0160	0.9756	0.6825
	2.0000	1.0000	2.0000	5.0000	1.5000	0.0160	0.
	0.3943	0.6184	1.7260	-0.0262	0.3425	0.5134	21.1099
	0.1365	0.1164	0.3737	0.1837	0.2540	0.2643	24.4266
44	100.0000	165.0000	75.0000	1.5000	0.0640	0.0842	0.0898
	2.0000	100.0000	2.0000	5.0000	1.5000	0.0640	0.
	0.8188	0.9048	1.6906	-0.0011	0.3751	0.6670	42.3444
	0.0506	0.0278	0.2478	0.4395	1.6830	0.2394	89.6764
45	0.1000	165.0000	60.0000	1.5000	0.0010	0.9975	0.6190
	4.0000	0.1000	4.0000	5.0000	1.5000	0.0010	0.
	0.4591	0.6750	1.8041	0.0050	0.7883	0.7767	29.3320
	0.0779	0.0587	0.1441	0.2839	1.2146	0.1393	107.9345
46	10.0000	135.0000	75.0000	1.5000	0.0040	0.7808	0.3633
	4.0000	10.0000	4.0000	5.0000	1.5000	0.0040	0.
	0.7314	0.8533	1.9979	-0.0424	0.3494	0.7057	39.9835
	0.0965	0.0567	0.2707	0.2822	0.3644	0.1915	39.1466

The over-all data format is:

Run No.	Ω_s^2	θ_i	ϕ_i	σ_s/d	ϵ_s/E_i	$e^{-a'\left(\frac{\omega_n \sigma}{V_i}\right)^2}$	Predicted $\overline{E_\ell/E_i}$
	μ_s	Ω_B^2	μ_B	FC	σ_B/d	ϵ_b/E_i	E_w/E_i
	$\overline{E_g/E_i}$	$\overline{V}$	$\overline{\sigma_z}$	$\overline{\sigma_L}$	$\overline{\sigma_t}$	$\overline{\cos\ \theta_f}$	$\overline{\lvert\phi_f\rvert}$
	$S(E_g/E_i)$	$S(V)$	$S(\sigma_z)$	$S(\sigma_L)$	$S(\sigma_t)$	$S(\cos\ \theta_f)$	$S(\phi_f)$
47	1.0000	120.0000	75.0000	1.2500	0.0010	0.9830	0.3171
	4.0000	1.0000	4.0000	5.0000	1.2500	0.0010	0.
	0.7315	0.8519	2.1609	-0.1261	0.3579	0.5805	48.4619
	0.1276	0.0758	0.4102	0.2848	0.3193	0.2051	35.4703
48	100.0000	150.0000	60.0000	1.2500	0.0040	0.1793	0.1005
	4.0000	100.0000	4.0000	5.0000	1.2500	0.0040	0.
	0.9148	0.9563	1.8482	-0.0096	0.8423	0.7345	22.4707
	0.0391	0.0205	0.1925	0.4196	0.9327	0.1668	107.0757
49	0.1000	135.0000	60.0000	1.5000	0.0010	0.9975	0.6314
	2.0000	0.1000	2.0000	5.0000	1.5000	0.0010	0.
	0.3754	0.6394	1.8592	-0.0409	0.5393	0.6835	42.6681
	0.1885	0.1170	0.4161	0.2100	0.3604	0.2134	54.5798
50	10.0000	165.0000	75.0000	1.5000	0.0040	0.7808	0.6805
	2.0000	10.0000	2.0000	5.0000	1.5000	0.0040	0.
	0.4251	0.6486	1.8068	-0.0004	0.6277	0.7793	49.7178
	0.0857	0.0667	0.1428	0.2713	1.0724	0.1380	94.1813
51	1.0000	150.0000	75.0000	1.2500	0.0010	0.9830	0.7587
	2.0000	1.0000	2.0000	5.0000	1.2500	0.0010	0.
	0.2549	0.5457	1.7028	0.0265	0.8946	0.7825	37.0384
	0.2222	0.1734	0.4180	0.1876	0.5076	0.1801	101.4317
52	100.0000	120.0000	60.0000	1.2500	0.0040	0.1793	0.0823
	2.0000	100.0000	2.0000	5.0000	1.2500	0.0040	0.
	0.9447	0.9717	2.3631	-0.1133	0.4274	0.6815	36.6673
	0.0451	0.0234	0.4896	0.2932	0.3925	0.2448	42.8927
53	0.1000	120.0000	75.0000	1.2500	0.0160	0.9983	0.3613
	4.0000	0.1000	4.0000	5.0000	1.2500	0.0160	0.
	0.7162	0.8436	2.0515	-0.0893	0.3080	0.5258	42.0613
	0.1130	0.0674	0.5244	0.2740	0.2627	0.2622	28.5260
54	10.0000	150.0000	60.0000	1.2500	0.0640	0.8421	0.5482
	4.0000	10.0000	4.0000	5.0000	1.2500	0.0640	0.
	0.3088	0.5796	1.5391	-0.0147	0.8343	0.5253	25.6911
	0.1602	0.1118	0.3594	0.3281	0.6383	0.2800	92.4463

55	1.0000	165.0000	60.0000	1.5000	0.0160	0.9756	0.6396
	4.0000	1.0000	4.0000	5.0000	1.5000	0.0160	0.
	0.4528	0.6701	1.7380	-0.0019	0.4780	0.7128	47.0251
	0.0839	0.0632	0.1940	0.3124	1.1990	0.1875	89.9241
56	100.0000	135.0000	75.0000	1.5000	0.0640	0.0842	0.0553
	4.0000	100.0000	4.0000	5.0000	1.5000	0.0640	0.
	0.8743	0.9639	1.8382	-0.0311	0.3693	0.6277	38.5138
	0.2160	0.0259	0.4628	0.3941	0.4804	0.3026	50.6596
57	0.1000	150.0000	75.0000	1.5000	0.0040	0.9975	0.5633
	4.0000	0.1000	4.0000	5.0000	1.5000	0.0040	0.
	0.5356	0.7288	1.8666	-0.0155	0.5212	0.7505	41.8711
	0.0982	0.0670	0.2002	0.2925	0.5969	0.1735	77.6614
58	10.0000	120.0000	60.0000	1.5000	0.0010	0.7808	0.2534
	4.0000	10.0000	4.0000	5.0000	1.5000	0.0010	0.
	0.8242	0.9063	2.2689	-0.0756	0.2886	0.6345	26.4298
	0.0941	0.0527	0.4141	0.2008	0.2645	0.2071	22.9306
59	1.0000	135.0000	60.0000	1.2500	0.0040	0.9830	0.4521
	4.0000	1.0000	4.0000	5.0000	1.2500	0.0040	0.
	0.5584	0.7415	1.9750	-0.0605	0.6848	0.6894	51.0551
	0.1366	0.0924	0.3311	0.3088	0.5311	0.2342	79.0945
60	100.0000	165.0000	75.0000	1.2500	0.0010	0.1793	0.1111
	4.0000	100.0000	4.0000	5.0000	1.2500	0.0010	0.
	0.8958	0.9462	1.7550	-0.0024	1.0794	0.7293	63.6069
	0.0406	0.0216	0.2010	0.4481	1.6676	0.1942	110.5735
61	0.1000	165.0000	60.0000	1.2500	0.0640	0.9983	0.9979
	2.0000	0.1000	2.0000	5.0000	1.2500	0.0640	0.
	0.0260	0.3427	1.1652	0.0378	0.9693	0.7184	54.4581
	0.0515	0.0485	0.3437	0.2029	0.1876	0.3076	72.6438
62	10.0000	135.0000	75.0000	1.2500	0.0160	0.8421	0.5639
	2.0000	10.0000	2.0000	5.0000	1.2500	0.0160	0.
	0.4336	0.6485	1.8443	-0.0407	0.5144	0.5970	46.3007
	0.1538	0.1187	0.4380	0.2630	0.4087	0.3097	61.9731
63	1.0000	120.0000	75.0000	1.5000	0.0640	0.9756	0.9787
	2.0000	1.0000	2.0000	5.0000	1.5000	0.0640	0.
	-0.	-0.	1.0000	-0.	1.0000	-0.	-0.
	-0.	-0.	-0.	-0.	-0.	-0.	-0.
64	100.0000	150.0000	60.0000	1.5000	0.0160	0.0842	0.0697
	2.0000	100.0000	2.0000	5.0000	1.5000	0.0160	0.
	0.9334	0.9661	1.8799	-0.0121	0.4177	0.7620	23.0508
	0.0359	0.0187	0.2157	0.3734	0.7457	0.1869	76.7217
65	9.1900	135.0000	60.0000	1.6200	0.0451	0.7670	0.1815
	14.6800	9.1900	14.6800	5.0000	1.6200	0.0451	0.
	0.8685	0.9321	1.8727	-0.0108	0.2230	0.6171	22.3400
	0.0484	0.0261	0.0915	0.2971	0.4093	0.4093	37.1900

The over-all data format is:

Run No.	Ω_s^2	θ_i	ϕ_i	σ_s/d	ϵ_s/E_i	$e^{-a'\left(\frac{\omega_n \sigma}{V_i}\right)^2}$	Predicted $\overline{E_\ell/E_i}$
	μ_s	Ω_B^2	μ_B	FC	σ_B/d	ϵ_b/E_i	E_w/E_i
	$\overline{E_g/E_i}$	$\overline{V}$	$\overline{\sigma_z}$	$\overline{\sigma_L}$	$\overline{\sigma_t}$	$\overline{\cos\ \theta_f}$	$\overline{\lvert\phi_f\rvert}$
	$S(E_g/E_i)$	$S(V)$	$S(\sigma_z)$	$S(\sigma_L)$	$S(\sigma_t)$	$S(\cos\ \theta_f)$	$S(\phi_f)$
66	2.3200	135.0000	60.0000	1.6200	0.0113	0.9352	0.1738
	14.6800	2.3200	14.6800	5.0000	1.6200	0.0113	0.
	0.8868	0.9415	2.0121	-0.0230	0.2590	0.7156	23.7000
	0.0398	0.0212	0.2787	0.2527	0.3674	0.3674	340.8400
67	2.3200	165.0000	60.0000	1.6200	0.0113	0.9352	0.2274
	14.6800	2.3200	14.6800	5.0000	1.6200	0.0113	0.
	0.8236	0.9074	1.8367	-0.0019	0.3785	0.8082	45.2200
	0.0378	0.0209	0.1228	0.3549	1.3636	10.3636	880.3000
68	0.5800	135.0000	60.0000	1.6200	0.0028	0.9834	0.1702
	14.6800	0.5800	14.6800	5.0000	1.6200	0.0028	0.
	0.8830	0.9395	2.0516	-0.0357	0.3434	0.7436	31.9800
	0.0401	0.0214	0.2802	0.2667	0.4012	0.4012	430.9700
69	0.5800	165.0000	60.0000	1.6200	0.0028	0.9834	0.2299
	14.6800	0.5800	14.6800	5.0000	1.6200	0.0028	0.
	0.8264	0.9089	1.8234	-0.0025	0.5378	0.7953	49.5000
	0.0335	0.0185	0.1332	0.3034	1.4355	10.4355	930.5800
70	0.1450	135.0000	60.0000	1.6200	0.0007	0.9958	0.1692
	14.6800	0.1450	14.6800	5.0000	1.6200	0.0007	0.
	0.8708	0.9328	2.0695	-0.0533	0.4765	0.7563	20.3700
	0.0460	0.0246	0.2518	0.3740	0.4965	0.4965	750.3000
71	47.2000	135.0000	60.0000	1.7200	0.1383	0.2152	0.7896
	2.9100	47.2000	2.9100	5.0000	1.7200	0.1383	0.
	0.4554	0.6625	1.5775	0.0061	0.2712	0.4084	21.8500
	0.1968	0.1568	0.4981	0.2029	0.3794	0.3794	280.4000
72	11.8000	135.0000	60.0000	1.7200	0.0346	0.6811	0.5701
	2.9100	11.8000	2.9100	5.0000	1.7200	0.0346	0.
	0.5804	0.7579	1.7247	-0.0144	0.1936	0.5124	18.0000
	0.1232	0.0823	0.3993	0.2020	0.2598	0.2598	200.5800
73	11.8000	165.0000	60.0000	1.7200	0.0346	0.6811	0.5999
	2.9100	11.8000	2.9100	5.0000	1.7200	0.0346	0.
	0.3605	0.5944	1.6925	-0.0016	0.2506	0.6689	22.2900
	0.1067	0.0907	0.3176	0.2596	0.9786	0.9786	790.7700

```
74    2.9500 135.0000  60.0000   1.7200   0.0087   0.9085   0.5344
      2.9100   2.9500   2.9100   5.0000   1.7200   0.0087   0.
      0.6047   0.7745   1.8913  -0.0160   0.2179   0.6303  18.2800
      0.1077   0.0707   0.2544   0.1640   0.2292   0.2292 170.4100

75    2.9500 165.0000  60.0000   1.7200   0.0087   0.9085   0.7013
      2.9100   2.9500   2.9100   5.0000   1.7200   0.0087   0.
      0.3934   0.6228   1.8316  -0.0008   0.3346   0.8033  23.5500
      0.0931   0.0758   0.1380   0.2322   0.8912   0.8912 840.9100

76    0.7370 135.0000  60.0000   1.7200   0.0022   0.9763   0.5379
      2.9100   0.7370   2.9100   5.0000   1.7200   0.0022   0.
      0.5978   0.7700   1.9667  -0.0257   0.2898   0.6836  20.7600
      0.1066   0.0703   0.2496   0.1769   0.0259   0.2591 210.4500

77   93.1000 135.0000  60.0000   1.8950   0.5770   0.0253   0.9546
      1.4700  93.1000   1.4700   5.0000   1.8950   0.5770   0.
     -0.      -0.      -0.       0.      -0.      -0.      -0.
     -0.      -0.      -0.      -0.      -0.      -0.       0.

78   23.2500 135.0000  60.0000   1.8950   0.1443   0.3992   0.9919
      1.4700  23.2500   1.4700   5.0000   1.8950   0.1443   0.
     -0.      -0.      -0.       0.      -0.      -0.      -0.
     -0.      -0.      -0.      -0.      -0.      -0.      -0.

79   23.2500 165.0000  60.0000   1.8950   0.1443   0.3992   0.9728
      1.4700  23.2500   1.4700   5.0000   1.8950   0.1443   0.
     -0.      -0.      -0.      -0.      -0.      -0.      -0.
     -0.      -0.      -0.      -0.      -0.      -0.      -0.

80    5.8200 135.0000  60.0000   1.8950   0.0361   0.7946   0.9592
      1.4700   5.8200   1.4700   5.0000   1.8950   0.0361   0.
      0.0797   0.6043   0.8746   0.0228   0.1629  -0.      -0.
     -0.       0.0651  -0.       0.0829  -0.       0.1003  80.3700

81    5.8200 165.0000  60.0000   1.8950   0.0361   0.7946   0.9929
      1.4700   5.8200   1.4700   5.0000   1.8950   0.0361   0.
      0.0488   0.3616   1.5863  -0.0425   0.3616  -0.      -0.
     -0.       0.1354  -0.       0.1413  -0.       0.4520 550.0800

82    1.4550 135.0000  60.0000   1.8950   0.0090   0.9441   0.7260
      1.4700   1.4550   1.4700   5.0000   1.8950   0.0090   0.
      0.4298   0.6529   1.5815  -0.0061   0.1829   0.4112  -0.
      0.0920   0.0705   0.2097   0.0788   0.0999   0.0999  70.8100

83    2.9100 135.0000  60.0000   1.8950   0.0180   0.8914   0.8656
      1.4700   2.9100   1.4700   5.0000   1.8950   0.0180   0.
      0.3436   0.6046   1.3077  -0.0088   0.2101   0.2176  -0.
      0.1003   0.0818   0.4183   0.0790   0.1216   0.1216  80.0800

84    0.1000 120.0000 105.0000   1.2500   0.0010   0.9983   0.2888
      2.0000   0.1000   2.0000   5.0000   1.2500   0.0010   3.1623
      0.8583  -0.0527   1.9232  -0.2599   0.7406   0.4616  79.3110
      0.3809   0.1416   0.7511   0.6335   0.3830   0.3755  59.8723
```

The over-all data format is:

Run No.	Ω_s^2	θ_i	ϕ_i	σ_s/d	ϵ_s/E_i	$e^{-a'\left(\frac{\omega_n \sigma}{V_i}\right)^2}$	Predicted $\overline{E_\ell/E_i}$
	μ_s	Ω_B^2	μ_B	FC	σ_B/d	ϵ_b/E_i	E_w/E_i
	$\overline{E_g/E_i}$	$\overline{V}$	$\overline{\sigma_z}$	$\overline{\sigma_L}$	$\overline{\sigma_t}$	$\overline{\cos \theta_f}$	$\overline{\lvert\phi_f\rvert}$
	$S(E_g/E_i)$	$S(V)$	$S(\sigma_z)$	$S(\sigma_L)$	$S(\sigma_t)$	$S(\cos \theta_f)$	$S(\phi_f)$
85	10.0000	150.0000	120.0000	1.2500	0.0040	0.8421	0.6587
	2.0000	10.0000	2.0000	5.0000	1.2500	0.0040	0.1000
	0.4879	0.5797	1.8446	-0.1411	0.6432	0.7315	89.1956
	0.1838	0.2080	0.3471	0.1818	0.4750	0.3006	71.9176
86	1.0000	165.0000	120.0000	1.5000	0.0010	0.9756	0.8065
	2.0000	1.0000	2.0000	5.0000	1.5000	0.0010	0.3162
	0.3340	1.0554	1.8285	-0.0790	0.4302	0.8002	112.2004
	0.1736	0.2751	0.1285	0.1860	1.0019	0.1241	76.5242
87	100.0000	135.0000	105.0000	1.5000	0.0040	0.0842	-0.5781
	2.0000	100.0000	2.0000	5.0000	1.5000	0.0040	1.0000
	1.0367	-0.0734	1.9939	0.1606	0.2311	0.7028	55.2295
	0.1062	0.2124	0.2714	0.2409	0.4593	0.1919	45.8727
88	0.1000	135.0000	120.0000	1.5000	0.0160	0.9975	0.4862
	4.0000	0.1000	4.0000	5.0000	1.5000	0.0160	0.1000
	0.6013	0.4514	1.8890	-0.1080	0.4340	0.6286	77.4723
	0.0873	0.0988	0.3561	0.1986	0.4888	0.2518	72.0826
89	10.0000	165.0000	105.0000	1.5000	0.0640	0.7808	-0.6832
	4.0000	10.0000	4.0000	5.0000	1.5000	0.0640	3.1623
	1.4097	0.1523	1.7607	0.1574	-0.3560	0.7348	55.9497
	0.7958	0.2959	0.1504	0.5182	1.7091	0.1452	68.6737
90	1.0000	150.0000	105.0000	1.2500	0.0160	0.9830	0.4348
	4.0000	1.0000	4.0000	5.0000	1.2500	0.0160	1.0000
	1.1505	0.9033	1.7379	0.1164	-0.2267	0.6390	53.6729
	0.4158	2.4948	0.2328	0.3430	0.8097	0.2016	44.3697
91	100.0000	120.0000	120.0000	1.2500	0.0640	0.1793	-0.1107
	4.0000	100.0000	4.0000	5.0000	1.2500	0.0640	0.3162
	0.8989	0.1201	2.2049	0.2486	0.3590	0.6025	63.2778
	0.1132	0.1344	0.5299	0.2588	0.3519	0.2649	38.4960
92	0.1000	165.0000	120.0000	1.2500	0.0040	0.9983	0.4634
	4.0000	0.1000	4.0000	5.0000	1.2500	0.0040	3.1623
	0.8526	-0.2537	1.4084	-0.1677	0.4604	0.3945	127.5595
	0.6124	1.0538	0.2154	0.3675	2.8994	0.2081	70.9899

93	10.0000	135.0000	105.0000	1.2500	0.0010	0.8421	0.3633
	4.0000	10.0000	4.0000	5.0000	1.2500	0.0010	0.1000
	0.5880	0.4337	1.9577	-0.1168	0.9493	0.6772	102.6922
	0.1332	0.1402	0.3398	0.3283	0.5404	0.2402	106.5563
94	1.0000	120.0000	105.0000	1.5000	0.0040	0.9756	0.3329
	4.0000	1.0000	4.0000	5.0000	1.5000	0.0040	0.3162
	0.6198	0.4516	2.5935	-0.0503	0.6843	0.7927	106.4110
	0.2629	0.3124	0.2891	0.1210	0.4005	0.1699	70.5000
95	100.0000	150.0000	120.0000	1.5000	0.0010	0.0842	-0.5855
	4.0000	100.0000	4.0000	5.0000	1.5000	0.0010	1.0000
	1.0211	-0.0422	1.9311	-0.1928	0.9681	0.8063	70.2155
	0.1924	0.3847	0.1314	0.3303	0.8392	0.1138	104.3964
96	0.1000	150.0000	105.0000	1.5000	0.0640	0.9975	0.9353
	2.0000	0.1000	2.0000	5.0000	1.5000	0.0640	0.1000
	0.2456	0.7941	1.7346	-0.1533	0.2989	0.6362	83.6239
	-0.	-0.	-0.	-0.	-0.	-0.	-0.
97	10.0000	120.0000	120.0000	1.5000	0.0160	0.7808	-0.8340
	2.0000	10.0000	2.0000	5.0000	1.5000	0.0160	3.1623
	1.5860	1.0084	2.0347	0.2083	-0.0213	0.5174	61.7552
	0.6909	1.1889	0.5434	0.1906	0.1083	0.2717	12.3971
98	1.0000	135.0000	120.0000	1.2500	0.0640	0.9830	0.4893
	2.0000	1.0000	2.0000	5.0000	1.2500	0.0640	1.0000
	0.8288	0.3423	1.9417	0.0281	0.6693	0.6659	54.9256
	0.4798	0.9597	0.3511	0.5454	0.3116	0.2483	62.3203
99	100.0000	165.0000	105.0000	1.2500	0.0160	0.1793	-0.0356
	2.0000	100.0000	2.0000	5.0000	1.2500	0.0160	0.3162
	0.8684	0.1563	1.8194	-0.2270	1.4704	0.7915	151.6508
	0.0994	0.1180	0.1868	0.3040	1.5012	0.1804	93.3098
100	3.1620	142.5000	112.5000	1.3750	0.0080	0.9364	0.5943
	2.8180	3.1620	2.8180	5.0000	1.3750	0.0080	0.
	0.3879	0.6113	1.9252	0.0114	0.9273	0.7340	44.3370
	0.1446	0.1195	0.2063	0.2684	0.5452	0.1636	102.4637
101	0.1000	142.5000	112.5000	1.2500	0.0010	0.9983	0.7992
	1.0000	0.1000	1.0000	5.0000	1.2500	0.0010	0.
	0.2698	0.4968	1.9004	-0.0161	0.5003	0.7143	63.2583
	0.1585	0.1522	0.2323	0.1089	0.2712	0.1843	28.3795
102	1.0000	142.5000	112.5000	1.5000	0.0040	0.9756	0.5081
	4.0000	1.0000	4.0000	5.0000	1.5000	0.0040	0.
	0.5166	0.7127	1.9204	0.0468	0.9043	0.7302	41.3384
	0.1311	0.0934	0.2011	0.2829	0.6461	0.1596	108.3826
103	0.1000	142.5000	112.5000	1.2500	0.0010	0.9983	0.5115
	4.0000	0.1000	4.0000	5.0000	1.2500	0.0010	0.
	0.4605	0.6723	1.9590	-0.0251	0.8757	0.7608	45.0224
	0.1317	0.0932	0.1679	0.1686	0.6679	0.1332	107.6293

The over-all data format is:

Run No.	Ω_s^2	θ_i	ϕ_i	σ_s/d	ϵ_s/E_i	$e^{-a'\left(\frac{\omega_n \sigma}{V_i}\right)^2}$	Predicted $\overline{E_\ell/E_i}$
	μ_s	Ω_B^2	μ_B	FC	σ_B/d	ϵ_b/E_i	E_w/E_i
	$\overline{E_g/E_i}$	$\overline{V}$	$\overline{\sigma_z}$	$\overline{\sigma_L}$	$\overline{\sigma_t}$	$\overline{\cos\ \theta_f}$	$\overline{\lvert\phi_f\rvert}$
	$S(E_g/E_i)$	$S(V)$	$S(\sigma_z)$	$S(\sigma_L)$	$S(\sigma_t)$	$S(\cos\ \theta_f)$	$S(\phi_f)$
104	3.1620	142.5000	112.5000	1.3750	0.0080	0.9364	0.5943
	2.8180	3.1620	2.8180	5.0000	1.3750	0.0080	0.
	0.4758	0.6844	1.9516	-0.0213	0.6206	0.7549	88.0035
	0.1174	0.0867	0.2746	0.2453	0.4991	0.2178	71.6279
105	0.1000	142.5000	112.5000	1.2500	0.0010	0.9983	0.7992
	1.0000	0.1000	1.0000	5.0000	1.2500	0.0010	0.
	0.0521	0.2222	1.8864	-0.0595	0.7887	0.7032	89.4510
	0.0278	0.0573	0.1770	0.0452	0.0799	0.1404	14.9254
106	1.0000	142.5000	112.5000	1.5000	0.0040	0.9756	0.5081
	4.0000	1.0000	4.0000	5.0000	1.5000	0.0040	0.
	0.6085	0.7777	1.9593	-0.0124	0.5127	0.7611	86.1686
	0.0934	0.0617	0.2405	0.2802	0.4741	0.1908	64.5695
107	0.1000	142.5000	112.5000	1.2500	0.0010	0.9983	0.5115
	4.0000	0.1000	4.0000	5.0000	1.2500	0.0010	0.
	0.3800	0.6096	1.9482	-0.1104	1.0093	0.7523	106.4253
	0.1168	0.0919	0.2134	0.1888	0.5863	0.1693	109.7740
108	0.0100	142.5000	112.5000	1.5000	0.0002	0.9998	0.7992
	1.0000	0.0100	1.0000	5.0000	1.5000	0.0002	0.
	0.2174	0.4370	1.9189	-0.0292	0.5936	0.7290	62.2369
	0.1535	0.1646	0.2886	0.0953	0.2253	0.2290	30.1855
109	10.0000	142.5000	112.5000	1.5000	0.0160	0.7808	0.6709
	1.0000	10.0000	1.0000	5.0000	1.5000	0.0160	0.
	0.5737	0.7505	1.9175	0.0069	0.9949	0.7279	40.8584
	0.1578	0.1022	0.1544	0.2577	0.7080	0.1225	105.8194
110	100.0000	142.5000	112.5000	1.5000	0.0640	0.0842	0.0876
	1.0000	100.0000	1.0000	5.0000	1.5000	0.0640	0.
	0.9297	0.9641	2.1001	-0.1337	0.6850	0.8727	81.8756
	0.0097	0.0051	0.0679	0.4005	0.0930	0.0538	61.4253
111	0.0100	142.5000	112.5000	1.5000	0.0640	0.9998	1.0000
	1.0000	0.0100	1.0000	5.0000	1.5000	0.0640	0.
	0.	0.	0.	0.	0.	0.	0.
	-0.	-0.	-0.	-0.	-0.	-0.	-0.

```
112 100.0000 142.5000 112.5000   1.5000   0.0002   0.0842   0.0431
      4.0000 100.0000   4.0000   5.0000   1.5000   0.0002   0.
      0.8582  -0.      -0.      -0.      -0.      -0.      -0.
     -0.      -0.      -0.      -0.      -0.      -0.      -0.

113  10.0000 142.5000 112.5000   1.5000   0.0002   0.7808   0.6242
      1.0000  10.0000   1.0000   5.0000   1.5000   0.0002   0.
      0.6178   0.7812   1.9792   0.0347   1.0440   0.7768  -4.2053
      0.1419   0.0875   0.2064   0.1957   0.7130   0.1637  84.4268

114   0.0100 142.5000 112.5000   1.5000   0.0160   0.9998   0.5498
      4.0000   0.0100   4.0000   5.0000   1.5000   0.0160   0.
      0.5103   0.7069   1.7656   0.0921   0.8270   0.6074  85.4107
      0.1442   0.1015   0.2853   0.3253   0.7302   0.2264 104.5553

115   0.0100 142.5000 112.5000   1.5000   0.0002   0.9998   0.5115
      4.0000   0.0100   4.0000   5.0000   1.5000   0.0002   0.
      0.4617   0.6737   2.0117  -0.0200   0.9150   0.8026  23.7448
      0.1261   0.0896   0.2530   0.1312   0.6240   0.2007 115.3626

116   3.1620 142.5000 112.5000   1.3750   0.0080   0.9364   0.5687
      2.8184   3.1620   2.8184   5.0000   1.3750   0.0080   0.1000
      0.4316   0.6491   2.0043  -0.0420   0.7650   0.7968  54.7387
      0.1326   0.1019   0.2111   0.2614   0.4341   0.1675  88.1212

117   3.1620 142.5000 112.5000   1.3750   0.0080   0.9364   0.5135
      2.8184   3.1620   2.8184   5.0000   1.3750   0.0080   0.3162
      0.4308   0.6448   1.9956  -0.0107   0.8706   0.7899  65.9325
      0.1623   0.1231   0.2248   0.3007   0.4160   0.1784  95.1083

118   0.1000 142.5000 112.5000   1.3750   0.0080   0.9979   0.6278
      2.8184   0.1000   2.8184   5.0000   1.3750   0.0080   0.1000
      0.3537   0.5794   1.7157   0.0762   0.9535   0.5678  46.1677
      0.1550   0.1373   0.3955   0.2397   0.6565   0.3138 107.0489

119   1.0000 135.0000  75.0000   1.5000   0.0160   0.9756   0.6825
      2.0000   1.0000   2.0000   5.0000   1.5000   0.0160   0.
      0.3845   0.6144   1.6681   0.1318   0.3972   0.4724   8.1674
      0.1227   0.0991   0.3033   0.2307   0.2715   0.2145  32.2942

120   1.0000 135.0000 105.0000   1.5000   0.0160   0.9756   0.6825
      2.0000   1.0000   2.0000   5.0000   1.5000   0.0160   0.
      0.3169   0.5496   1.7863   0.1149   0.6155   0.5560  55.7787
      0.1343   0.1245   0.4927   0.2671   0.3035   0.3484  54.0746

121   1.0000 135.0000  70.0000   1.5000   0.0160   0.9756   0.6825
      2.0000   1.0000   2.0000   5.0000   1.5000   0.0160   0.
      0.3611   0.5914   1.4533   0.0271   0.2886   0.3205  20.9448
      0.1279   0.1114   0.4209   0.1834   0.2091   0.2976  20.6973

122   1.0000 135.0000  82.5000   1.5000   0.0160   0.9756   0.6825
      2.0000   1.0000   2.0000   5.0000   1.5000   0.0160   0.
      0.4067   0.6286   1.5607   0.0630   0.2319   0.3964  29.6985
      0.1318   0.1096   0.1953   0.1651   0.1733   0.1381  17.1207
```

The over-all data format is:

Run No.	Ω_s^2	θ_i	ϕ_i	σ_s/d	ϵ_s/E_i	$e^{-a'\left(\frac{\omega_n \sigma}{V_i}\right)^2}$	Predicted $\overline{E_\ell/E_i}$
	μ_s	Ω_B^2	μ_B	FC	σ_B/d	ϵ_b/E_i	E_w/E_i
	$\overline{E_g/E_i}$	$\overline{V}$	$\overline{\sigma_z}$	$\overline{\sigma_L}$	$\overline{\sigma_t}$	$\overline{\cos\ \theta_f}$	$\overline{\lvert\phi_f\rvert}$
	$S(E_g/E_i)$	$S(V)$	$S(\sigma_z)$	$S(\sigma_L)$	$S(\sigma_t)$	$S(\cos\ \theta_f)$	$S(\phi_f)$
123	1.0000	135.0000	50.0000	1.5000	0.0160	0.9756	0.6825
	2.0000	1.0000	2.0000	5.0000	1.5000	0.0160	0.
	0.4117	0.6391	1.4749	0.0243	0.2699	0.3358	0.2212
	0.1422	0.1073	0.3744	0.2629	0.1877	0.2648	25.4932
124	1.0000	135.0000	70.2000	1.5000	0.0160	0.9756	0.6825
	2.0000	1.0000	2.0000	5.0000	1.5000	0.0160	0.
	0.3612	0.5926	1.6772	0.1434	0.4161	0.4788	1.6038
	0.1300	0.1089	0.2918	0.2164	0.2600	0.2064	30.8678
125	1.0000	135.0000	80.3000	1.5000	0.0160	0.9756	0.6825
	2.0000	1.0000	2.0000	5.0000	1.5000	0.0160	0.
	0.3776	0.6057	1.6321	0.1333	0.4450	0.4470	7.0649
	0.1484	0.1236	0.3730	0.2390	0.3451	0.2638	38.8315
126	1.0000	135.0000	45.0000	1.5000	0.0160	0.9756	0.6825
	2.0000	1.0000	2.0000	5.0000	1.5000	0.0160	0.
	0.3517	0.5880	1.4364	0.0231	0.2911	0.3086	-2.2760
	0.0987	0.0845	0.4386	0.1677	0.1412	0.3101	18.9054
127	1.0000	135.0000	50.0000	1.5000	0.0160	0.9756	0.6825
	2.0000	1.0000	2.0000	5.0000	1.5000	0.0160	0.
	0.3582	0.5983	1.5780	0.0309	0.2805	0.4087	1.7382
	0.1125	0.0922	0.2808	0.1535	0.1516	0.1986	17.8402
128	1.0000	135.0000	60.0000	1.5000	0.0160	0.9756	0.6825
	2.0000	1.0000	2.0000	5.0000	1.5000	0.0160	0.
	0.3913	0.6187	1.5426	0.0457	0.2467	0.3837	9.6780
	0.1353	0.1109	0.3159	0.1358	0.1805	0.2234	15.7247
129	1.0000	135.0000	75.0000	1.5000	0.0160	0.9756	0.6825
	2.0000	1.0000	2.0000	5.0000	1.5000	0.0160	0.
	0.4232	0.6423	1.5269	0.0548	0.2113	0.3725	23.9946
	0.1314	0.1064	0.3397	0.1440	0.1716	0.2402	15.3137
130	1.0000	135.0000	67.5000	1.5000	0.0160	0.9756	0.6825
	2.0000	1.0000	2.0000	5.0000	1.5000	0.0160	0.
	0.4108	0.6323	1.5399	0.0531	0.2222	0.3818	16.3790
	0.1364	0.1121	0.3021	0.1375	0.1847	0.2136	14.3351

131	3.1620	142.5000	112.5000	1.3750	0.0080	0.9364	0.5862
	2.8184	3.1620	2.8184	5.0000	1.3750	0.0080	0.0316
	0.4498	0.6668	1.9474	0.0192	0.6999	0.7516	83.3470
	0.0949	0.0719	0.2741	0.2604	0.4743	0.2175	83.9569
132	3.1620	142.5000	112.5000	1.3750	0.0080	0.9364	0.5687
	2.8184	3.1620	2.8184	5.0000	1.3750	0.0080	0.1000
	0.4350	0.6550	1.9340	0.0245	0.7362	0.7410	40.5804
	0.1034	0.0778	0.2837	0.2675	0.4602	0.2251	80.0561
133	3.1620	142.5000	112.5000	1.3750	0.0080	0.9364	0.3387
	2.8184	3.1620	2.8184	5.0000	1.3750	0.0080	1.0000
	0.3179	0.5453	1.8747	0.0402	0.8816	0.6940	50.1148
	0.1631	0.1511	0.2337	0.2797	0.4119	0.1854	78.2937
134	3.1620	142.5000	112.5000	1.3750	0.0080	0.9364	-0.2139
	2.8184	3.1620	2.8184	5.0000	1.3750	0.0080	3.1623
	0.8820	0.8600	1.7450	0.1711	0.8778	0.5910	37.3620
	0.6025	0.3775	0.2508	0.4357	0.7138	0.1989	83.0646
135	3.1620	142.5000	112.5000	1.3750	0.0080	0.9364	0.5135
	2.8184	3.1620	2.8184	5.0000	1.3750	0.0080	0.3162
	0.3889	0.6121	1.8727	0.0353	0.7919	0.6924	43.4554
	0.1534	0.1204	0.2898	0.2941	0.4424	0.2299	76.9310
136	1.0000	135.0000	45.0000	1.5000	0.0160	0.9756	0.6479
	2.0000	1.0000	2.0000	5.0000	1.5000	0.0160	0.
	0.3548	0.5930	1.7898	0.0337	0.4824	0.5585	-5.7499
	0.0670	0.0578	0.3535	0.2953	0.1105	0.2499	35.9403
137	1.0000	135.0000	50.0000	1.5000	0.0160	0.9756	0.6479
	2.0000	1.0000	2.0000	5.0000	1.5000	0.0160	0.
	0.3464	0.5857	1.7936	0.0447	0.4783	0.5611	-4.7872
	0.0691	0.0596	0.2873	0.2843	0.1259	0.2032	35.6109
138	1.0000	135.0000	60.0000	1.5000	0.0160	0.9756	0.6479
	2.0000	1.0000	2.0000	5.0000	1.5000	0.0160	0.
	0.3243	0.5660	1.8321	0.0703	0.4945	0.5884	-1.9798
	0.0719	0.0641	0.1724	0.2389	0.2047	0.1219	38.0793
139	1.0000	135.0000	60.0000	1.5000	0.0160	0.9756	0.6479
	2.0000	1.0000	2.0000	5.0000	1.5000	0.0160	0.
	0.3243	0.5660	1.8321	0.0703	0.4945	0.5884	-1.9798
	0.0719	0.0641	0.1724	0.2389	0.2047	0.1219	38.0793
140	3.1620	142.5000	112.5000	1.3750	0.0080	0.9364	0.5843
	2.8184	3.1620	2.8184	5.0000	1.3750	0.0080	0.
	0.3854	0.6146	1.8073	0.0030	0.9111	0.6405	16.7120
	0.1730	0.1730	0.2920	0.2621	0.6647	0.2317	102.5463
141	3.1620	142.5000	60.0000	1.3750	0.0080	0.9364	0.5843
	2.8184	3.1620	2.8184	5.0000	1.3750	0.0080	0.
	0.4131	0.5869	1.8203	-0.0098	0.9557	0.6508	67.2176
	0.1820	0.1820	0.2900	0.2459	0.7113	0.2301	104.2821

The over-all data format is:

Run No.	Ω_s^2	θ_i	ϕ_i	σ_s/d	ϵ_s/E_i	$e^{-a'\left(\frac{\omega_n \sigma}{V_i}\right)^2}$	Predicted $\overline{E_\ell/E_i}$
	μ_s	Ω_B^2	μ_B	FC	σ_B/d	ϵ_b/E_i	E_w/E_i
	$\overline{E_g/E_i}$	$\overline{V}$	$\overline{\sigma_z}$	$\overline{\sigma_L}$	$\overline{\sigma_t}$	$\overline{\cos\ \theta_f}$	$\overline{\lvert\phi_f\rvert}$
	$S(E_g/E_i)$	$S(V)$	$S(\sigma_z)$	$S(\sigma_L)$	$S(\sigma_t)$	$S(\cos\ \theta_f)$	$S(\phi_f)$
142	3.1620	142.5000	112.5000	1.3750	0.0080	0.9364	0.6141
	2.8184	3.1620	2.8184	5.0000	1.3750	0.0080	0.
	0.5495	0.4505	1.8530	-0.0078	0.1619	0.6767	69.2130
	0.0941	0.0941	0.1668	0.1345	0.1951	0.1323	15.4851
143	3.1620	142.5000	112.5000	1.3750	0.0080	0.9364	0.5794
	2.8184	3.1620	2.8184	5.0000	1.3750	0.0080	0.
	0.3643	0.6357	1.9014	-0.2098	0.9516	0.7151	178.7142
	0.2021	0.2021	0.1095	0.1550	0.5927	0.0869	59.2478
144	3.1620	142.5000	112.5000	1.3750	0.0080	0.9364	0.5943
	2.8184	3.1620	2.8184	5.0000	1.3750	0.0080	0.
	0.5174	0.4826	1.7757	-0.0687	0.1960	0.6154	77.0301
	0.0910	0.0910	0.1838	0.2243	0.2488	0.1458	28.5094
145	3.1620	142.5000	112.5000	1.3750	0.0080	0.9364	0.5843
	2.8184	3.1620	2.8184	5.0000	1.3750	0.0080	0.
	0.3796	0.6204	1.8839	-0.1337	0.8581	0.7012	113.3883
	0.1490	0.1490	0.2835	0.1854	0.6136	0.2249	102.3984
146	3.1620	142.5000	112.5000	1.3750	0.0080	0.9364	0.5943
	2.8184	3.1620	2.8184	5.0000	1.3750	0.0080	0.
	0.5175	0.4825	1.7756	-0.0687	0.1959	0.6153	77.0311
	0.0910	0.0910	0.1838	0.2243	0.2488	0.1458	28.5033
147	3.1620	142.5000	60.0000	1.3750	0.0080	0.9364	0.5843
	2.8184	3.1620	2.8184	5.0000	1.3750	0.0080	0.
	0.4471	0.5529	1.7415	-0.0019	0.5963	0.5833	10.3820
	0.1752	0.1752	0.3412	0.2608	0.6603	0.2707	92.9806
148	3.1620	142.5000	60.0000	1.3750	0.0080	0.9364	0.5943
	2.8184	3.1620	2.8184	5.0000	1.3750	0.0080	0.
	0.5424	0.4576	1.7477	0.0121	0.1334	0.5932	13.9650
	0.0842	0.0842	0.1638	0.2327	0.1669	0.1299	24.2309
149	3.1620	142.5000	60.0000	1.3750	0.0080	0.9364	0.6141
	2.8184	3.1620	2.8184	5.0000	1.3750	0.0080	0.
	0.5518	0.4482	1.8498	0.0073	0.1568	0.6742	13.4201
	0.0915	0.0915	0.1567	0.1395	0.1856	0.1243	16.0373

150	3.1620	142.5000	60.0000	1.3750	0.0080	0.9364	0.5794
	2.8184	3.1620	2.8184	5.0000	1.3750	0.0080	0.
	0.4001	0.5999	1.6523	0.2225	0.8043	0.5175	-86.0119
	0.2154	0.2154	0.2800	0.1702	0.7730	0.2221	66.1451
151	3.1620	142.5000	112.5000	1.3750	0.0080	0.9364	0.3387
	2.8184	3.1620	2.8184	5.0000	1.3750	0.0080	1.0000
	0.6796	0.6408	2.0883	0.0785	1.1395	0.8634	53.9795
	0.3484	0.6968	0.1824	0.3588	0.2047	0.1447	98.9209
152	3.1620	142.5000	112.5000	1.3750	0.0080	0.9364	0.3387
	2.8184	3.1620	2.8184	5.0000	1.3750	0.0080	1.0000
	0.6302	0.7396	1.9377	0.2222	0.8593	0.7439	27.8457
	0.4148	0.8296	0.1637	0.3412	0.3159	0.1298	69.7733
153	3.1620	142.5000	112.5000	1.3750	0.0080	0.9364	0.3387
	2.8184	3.1620	2.8184	5.0000	1.3750	0.0080	1.0000
	0.5790	0.8420	1.9377	0.2233	0.9925	0.7440	36.0296
	0.2648	0.5297	0.2948	0.3025	0.4180	0.2339	91.6558

REFERENCES

1. Oman, R. A., Bogan, A., Weiser, C., and Li, C. H., "Interactions of Gas Molecules with an Ideal Crystal Surface," AIAA J., Vol. 2, No. 10, pp. 1722-30, October 1964.

2. Oman, R. A., Bogan, A., and Li, C. H., "Research on Molecule-Surface Interaction: Part I — Theoretical Prediction of Momentum and Energy Accommodation for Hypervelocity Gas Particles on an Ideal Crystal Surface," Grumman Research Department Report RE-181J, September 1964. (Also published in Rarefied Gas Dynamics, de Leeuw, ed., Academic Press, 1965.)

3. Oman, R. A., and Calia, V., Research on Molecule-Surface Interaction: Part II — Experiments on the Formation of a Shock Tube Driven Molecular Beam, Grumman Research Department Memorandum RM-240, September 1964.

4. Prince, R. H., A Low Energy Nitrogen Ion Beam, UTIAS Technical Note No. 80, University of Toronto Institute for Aerospace Studies, May 1965.

5. Wachman, H. Y., "The Thermal Accommodation Coefficient: A Critical Survey," ARS J., Vol. 32, No. 1, p. 2, January 1962.

6. Hurlbut, F. C., On the Molecular Interactions Between Gases and Solids, University of California Technical Report HE-150-208, 1962.

7. Smith, J. N., Jr., and Saltsburg, H., "Recent Studies of Molecular Beam Scattering from Continuously Deposited Gold Films," General Atomic Report No. GA-5356, June 1964. (Also published in Rarefied Gas Dynamics, 1965.)

8. Hinchen, J. J., and Foley, W. M., "Scattering of Molecular Beams by Metallic Surfaces," United Aircraft Corporation Research Laboratories Report UAR-C117, July 1964. (Also published in Rarefied Gas Dynamics, 1965.)

9. French, J. B., "Continuum-Source Molecular Beams," AIAA J., Vol. 3, No. 6, pp. 993-1000, June 1965.

10. Knuth, E. L., "Supersonic Molecular Beams," Appl. Mech. Rev., Vol. 17, p. 751, 1964.

11. Anderson, J. B., Andres, R. P., and Fenn, J. B., "High Intensity and High Energy Molecular Beams," in Advances in Atomic and Molecular Physics, D. R. Bates and J. Estermann, ed., Academic Press, New York, 1965.

12. Treanor, C. E., "Vibrational Energy Transfer in High Energy Collisions," J. Chem. Phys., Vol. 43, No. 2, pp. 532-8, 15 July 1965.

13. Rapp, D., "Vibrational Energy Exchange in Quantum and Classical Mechanics," J. Chem. Phys., Vol. 40, No. 10, pp. 2813-18, 15 May 1963.

14. Schaaf, S. A., and Chambre, P. L., "Flow of Rarefied Gases," in High Speed Aerodynamics and Jet Propulsion, H. W. Emmons, ed., Princeton University Press, 1958, Vol. 3, Sec. H.

15. Cook, G. E., Satellite Drag Coefficients, Royal Aircraft Establishment Technical Report No. 65005, Farnborough Hants, Great Britain, January 1965.

16. Goodman, F. O., "On the Theory of Accommodation Coefficients V. Classical Theory of Thermal Accommodation and Trapping." (published in Rarefied Gas Dynamics, 1965.)

17. Marsh, T., The Free-Molecule Flow of a Polyatomic Gas, Cranfield College of Aeronautics Report No. 159, Cranfield, England, May 1963.

18. Goodman, F. O., "On the Theory of Accommodation Coefficients IV — Simple Distribution Function Theory of Gas-Solid Interaction Systems," J. Phys. Chem. Solids, December 1964.

19. Logan, R. M., and Stickney, R. E., "A Simple Classical Model for the Scattering of Gas Atoms from a Solid Surface," J. Chem. Phys., 44, January 1966.

20. Bogan, A., Jr., Tabulated Results of Calculated Molecule-Surface Interactions, Grumman Research Department Memorandum RM-237, July 1964.